

NASA/TM-2014-216622



## **Introduction to Analogy Between Wind Tunnels and Charged-Particle Accelerators**

*Vernon J. Rossow  
Ames Research Center  
Moffett Field, California*

---

**June 2014**

## The NASA STI Program Office . . . in Profile

Since its founding, NASA has been dedicated to the advancement of aeronautics and space science. The NASA Scientific and Technical Information (STI) Program Office plays a key part in helping NASA maintain this important role.

The NASA STI Program Office is operated by Langley Research Center, the Lead Center for NASA's scientific and technical information. The NASA STI Program Office provides access to the NASA STI Database, the largest collection of aeronautical and space science STI in the world. The Program Office is also NASA's institutional mechanism for disseminating the results of its research and development activities. These results are published by NASA in the NASA STI Report Series, which includes the following report types:

- **TECHNICAL PUBLICATION.** Reports of completed research or a major significant phase of research that present the results of NASA programs and include extensive data or theoretical analysis. Includes compilations of significant scientific and technical data and information deemed to be of continuing reference value. NASA's counterpart of peer-reviewed formal professional papers but has less stringent limitations on manuscript length and extent of graphic presentations.
- **TECHNICAL MEMORANDUM.** Scientific and technical findings that are preliminary or of specialized interest, e.g., quick release reports, working papers, and bibliographies that contain minimal annotation. Does not contain extensive analysis.
- **CONTRACTOR REPORT.** Scientific and technical findings by NASA-sponsored contractors and grantees.

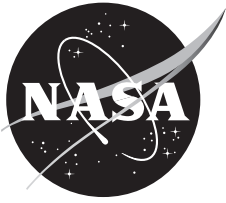
- **CONFERENCE PUBLICATION.** Collected papers from scientific and technical conferences, symposia, seminars, or other meetings sponsored or cosponsored by NASA.
- **SPECIAL PUBLICATION.** Scientific, technical, or historical information from NASA programs, projects, and missions, often concerned with subjects having substantial public interest.
- **TECHNICAL TRANSLATION.** English-language translations of foreign scientific and technical material pertinent to NASA's mission.

Specialized services that complement the STI Program Office's diverse offerings include creating custom thesauri, building customized databases, organizing and publishing research results . . . even providing videos.

For more information about the NASA STI program, see the following:

- Access the NASA STI program home page at <http://www.sti.nasa.gov>
- E-mail your question via the Internet to [help@sti.nasa.gov](mailto:help@sti.nasa.gov)
- Fax your question to the NASA STI Help Desk at 443-757-5803
- Telephone the NASA STI Help Desk at 443-757-5802
- Write to:  
NASA Center for AeroSpace Information (CASI)  
7115 Standard Drive  
Hanover, MD 21076-1320

NASA/TM-2014-216622



# **Introduction to Analogy Between Wind Tunnels and Charged-Particle Accelerators**

*Vernon J. Rossow  
Ames Research Center  
Moffett Field, California*

National Aeronautics and  
Space Administration

Ames Research Center  
Moffett Field, California 94035-1000

---

**June 2014**

## **Acknowledgments**

The author acknowledges and thanks Dr. U. Wienands of the Stanford Linear Accelerator (SLAC) organization near Palo Alto, CA for providing an insightful review of this paper. The author also thanks V. A. Delossantos for assistance with the preparation of the figures in this paper.

Available from:

NASA Center for Aerospace Information  
7115 Standard Drive  
Hanover, MD 21076-1320

National Technical Information Service  
5301 Shawnee Road  
Alexandria, VA 22312

## TABLE OF CONTENTS

LIST OF FIGURES .....	v
NOMENCLATURE .....	vii
SUMMARY .....	1
I. INTRODUCTION .....	2
II. EXAMPLES OF A SUBSONIC AND A SUPERSONIC WIND TUNNEL .....	5
III. NOISE PROPAGATION PATTERNS FOR SEVERAL VELOCITY REGIMES OF MOVING DISTURBANCES .....	7
A. Critical Velocity and Mach Number .....	7
B. Velocity Domains of a Moving Noise Source Relative to Earth's Atmosphere.....	8
C. Velocity Domains of Moving Electromagnetic Noise Source in Atmosphere of Charged Particles Like Electrons .....	13
IV. EQUATION OF STATE AND CRITICAL SPEED .....	13
A. Streams of Air .....	13
B. Stream of Electron Gas.....	16
V. DESIGN OF ONE-DIMENSIONAL CHANNELS FOR TRANSITION FROM SUBCRITICAL TO SUPERCRITICAL FLOW VELOCITIES—STREAM OF NEUTRAL GAS.....	19
A. Differential Equations .....	19
B. Effect of Variations in Size of Cross Section of Channel on Velocity and Mach Number Stream of Neutral Gas.....	21
C. Transition of Stream Velocities of Air from Less-Than to Greater-Than Critical .....	23
D. Overview of Channel Dynamics .....	24
E. Linearized Partial Differential Equations for Compressible Flow of Neutral Gas .....	25
F. Examples of Wind Tunnel Data At and Near Critical Velocity .....	25
G. Return-Flow Part of Wind Tunnel Circuits .....	26
VI. DESIGN OF ONE-DIMENSIONAL CHANNELS FOR TRANSITION FROM SUBCRITICAL TO SUPERCRITICAL FLOW VELOCITIES— STREAM OF ELECTRON GAS .....	27
A. Differential Equations .....	27
B. Effect of Variations in Size of Cross Section of Channel on Velocity and Mach Number .....	28
C. Return-Flow Part of Wind Tunnel Circuits .....	30
VII. MACH WAVES—A TOOL FOR THE ANALYSIS OF SUPERCRITICAL AERODYNAMIC FLOW FIELDS.....	31
A. Aerodynamic Problem in Need of Solution .....	31
B. Mach Waves—A Theoretical Relationship Between Stream Velocity, $V_1$ , and Small Flow-Turning Angle, $d\theta$ , When Gas Is Air .....	33
C. Analysis of Mach Wave for Small Angular Changes in Stream Angle.....	35
D. Use of Reservoir Conditions to Relate Flow-Field Parameters to Each Other for Integration of Mach Wave Relationship for Air .....	37

## TABLE OF CONTENTS (cont.)

E. Application of Differential Increment of Mach Waves to Prandtl-Meyer Expansion Fans .....	38
F. Method of Characteristics—Utilization of Mach Waves to Analyze Two- and Three-Dimensional Supercritical Flow Fields.....	40
VIII. ADAPTATION OF MACH WAVE CONCEPT FOR STREAMS OF AIR TO SUPERCRITICAL STREAMS OF ELECTRON GAS .....	42
A. Overview .....	42
B. Adaptation of Mach Wave Concept for Air to Electron Gas.....	43
C. Use of Reservoir Conditions for Electron Gas to Integrate Mach Wave Relationship.....	44
IX. OBSERVED STRUCTURE OF ROCKET-EXHAUST PLUME AS FUNCTION OF ALTITUDE.....	46
A. Background .....	46
B. Time-History of Rocket Exhaust Plume as Function of Altitude.....	46
X. CONCLUDING REMARKS.....	48
XI. REFERENCES .....	50
APPENDIX: DERIVATION OF ESTIMATE FOR PROPAGATION VELOCITY OF SMALL DISTURBANCE WAVES IN AN IDEALIZED ELECTRON GAS .....	52
A. Introduction .....	52
B. Derivation of Equation for Speed of Propagation of Small Disturbance Waves.....	56
C. Symbolic Ratio of Specific Heats, $\gamma_e$ , for Streams of Electron Gas .....	59

## LIST OF FIGURES

Figure 1.	Schematic diagram of Boeing Commercial Airplane Co.'s open-circuit non-return flow-through subsonic wind tunnel; test section is 9 feet by 9 feet in cross section and 14.5 feet in length. Reproduced from Penaranda and Freda (ref. 2), p. 111A. The facility is a flow-through device and does not have a flow-return part. ....5
Figure 2.	Schematic diagram of NASA Langley Research Center's Mach number 8 open-circuit non-return flow-through hypersonic wind tunnel. Test section is 18 inches in diameter and the usable diameter of the test stream is 4 to 14 inches in diameter depending on the pressure in the vacuum spheres at the time. Maximum run time = 1.5 min. Facility has a large amount of pumping and air-conditioning machinery that is not shown here. These important and mostly concrete and steel components are not shown because they do not require a unique design. (Penaranda and Freda, ref. 2, p. 269A.).....6
Figure 3.	Illustrations of patterns of sound waves as a function of time as generated by an object or aircraft as it flies through a gas like air at four different velocities. The quantity 'a' in the figure captions denotes the critical velocity of the gas through which the object is flying (in this figure, as for neutral gases, the critical velocity and the speed of sound, a, are the same) and the quantity 'V' denotes the velocity of the object relative to that of the gas, which is assumed to be stationary in the present examples.....9
Figure 4.	Diagram of a portion of wind tunnel circuit to illustrate how certain aspects of channel design must be made if the transition from subsonic to supersonic flow is to be accomplished. The transition is made at the smallest part of the throat of the nozzle where the stream Mach number goes through 1.0 on its way to a Mach number of 8.0. The expanding part of the channel downstream of the throat is designed to produce a uniform stream in the test section. This figure is a portion of the figure used to illustrate NASA Langley Research Center's Mach number 8 open-circuit non-return flow-through hypersonic wind tunnel (reproduced from page 269A of ref. 2). A more complete picture of the facility is shown in figure 2. ....23
Figure 5.	Comparison of predicted and measured lift-curve slope as taken in a transonic wind tunnel as a function of stream Mach number for two wing-body combinations when one wing is a clipped triangular wing-tip configuration with an aspect ratio of four, and the other is not, as indicated on the figure in plan view. (From figures G,2e and G,2f on pages 802-3 in ref. 9.).....26
Figure 6.	Diagram of a supersonic flow field around a single, smooth aerodynamic turn like the ones that often occur along wind tunnel walls or on the surfaces of aircraft (from fig. 14 of Courant and Friedrichs ref. 13). ....32
Figure 7.	Diagram of velocity components relative to entry and exit of a stream of air from a Mach wave (or small bundle of Mach waves) to show how the small-amplitude components perpendicular to the Mach wave simultaneously produce a change in the velocity, or an acceleration, $dV_n$ , of the stream component perpendicular to the Mach wave bundle, and thereby an angular turn, $d\theta$ , in the flow direction of the stream (refs. 11-14 and 21-26). ....34
Figure 8.	Centered modest-angle Prandtl-Meyer expansion fan for air (from ref. 13, Courant and Friedrichs, fig. 16, p. 277). ....39
Figure 9.	Complete or maximum theoretical centered angular expansion possible when stream around corner is composed of air with ratio of specific heats of 1.4 (from ref. 13, fig. 17, pp. 278; also see Liepmann and Puckett (ref. 12) p. 216ff). Note that if the turn in flow-direction angle exceeds the thermal energy available in the air (in this case, a temperature limit that allows only a 220.4° angular turn) it is labeled here by the word "cavitation" to indicate that turning angles do have a limit. In practice, maximum turn angles are usually limited by flow separation in the viscous boundary layers on the walls of wind tunnel nozzles and on aircraft lifting surfaces. ....40

## LIST OF FIGURES (cont.)

- Figure 10. Supersonic flow field at bend in duct as analyzed by method of characteristics. Example illustrates how two families of Mach waves interact with each other to develop the two-dimensional form of the flow fields (from ref. 13, fig. 21, p. 282).....41
- Figure 11. Reduced-size photograph of typical 30-in. by 8-ft worksheet used to carry out computations (refs. 24, 25) by use of the method of characteristics to determine the flow field around an axially symmetric ogive-cylinder of length/diameter ratio = 2.0, in an airstream moving at twice the speed of sound (Mach number = 2). Lines drawn are Mach waves used as part of the method of characteristics to compute the flow-field structure shown in the figure. Numbers on top or upper side of Mach wave intersections are local Mach number, and lower numbers are local stream angle. ....42
- Figure 12. Copy of figure 7 with revised labels (subscript 'e' added) to indicate that the figure and the text now apply to supercritical streams composed of electrons rather than air. Vectors and angles were not changed because they still apply in concept, but not necessarily in the same relative magnitudes.....43
- Figure A1. Diagram of a portion of the front view of theoretical mesh-spacing and electron distribution assumed for electron gas. Side and plan views are the same except for coordinate labels. Size of mesh and electron spacing are the same in all three directions, with an electron centered inside of each cube. ....53

## NOMENCLATURE

A	= cross-sectional area of channel
a	= velocity of propagation of small disturbance wave, or speed of sound, in air
$C_p$	= specific heat of air at constant pressure
$C_v$	= specific heat of air at constant volume
$d_e$	= distance between centers of electrons in electron gas, meters
e	= electron, or, electronic charge = $1.60207 \times 10^{-19}$ Coulomb
$1/4\pi K_0$	= $8.988 \times 10^9$ [(newton-m <sup>2</sup> )/(amp <sup>2</sup> -sec <sup>2</sup> )] = $8.988 \times 10^9$ [(volt-m)/(amp-sec)]
E	= internal energy
F	= force
p	= pressure
q	= dynamic pressure = $\rho U^2/2$
R	= universal gas constant = $1715 \text{ ft}^2/\text{sec}^2 \text{ } ^\circ\text{F}$
t	= time, seconds
T	= Temperature, degrees Fahrenheit or Kelvin
x	= horizontal distance, ft (m)
y, z	= distance in lateral and vertical directions, ft (m)
u, v, w	= velocity components in x, y, and z directions, ft/s (m/s)
U	= velocity of stream
$U_\infty$	= velocity of undisturbed stream
$\delta_w$	= displacement distance of electron from undisturbed location, meters
$\gamma$	= ratio of specific heats of air = $C_p/C_v$
$\theta$	= stream deflection angle, degrees
$\rho$	= density of gas, slugs/ft <sup>3</sup> (kg/m <sup>3</sup> )

### Subscripts

a	= item associated with air
e	= item associated with electron gas
$\infty$	= undisturbed stream



# INTRODUCTION TO ANALOGY BETWEEN WIND TUNNELS AND CHARGED-PARTICLE ACCELERATORS

Vernon J. Rossow<sup>1</sup>

Ames Research Center

## SUMMARY

A possibly improved method for the acceleration of charged particles to velocities greater than the critical velocity of their stream is studied by use of the analogy between a portion of the flow-field circuits used by supersonic wind tunnels and a similar portion of the flow-field circuit used by charged-particle accelerators. The study was motivated by the observation that streams in supersonic wind tunnels achieve their high velocities by utilization of expansion forces provided by upstream parts of the airstream to drive the downstream parts of the stream to higher velocities. Utilization of pressure forces within upstream parts of the stream to accelerate downstream parts has enabled the streams of supersonic wind tunnels to exceed their critical (or sonic) velocity of their streams by considerable amounts. It is now well known that the success of such a process requires a specially shaped aerodynamic channel and pumping systems if the airstream is to achieve velocities in excess of critical, in which case wind tunnels are referred to as being supersonic.

The purpose of this paper is to suggest that some of the methodologies and analyses used in developing theoretical models of supersonic flow fields may have application to the design and analysis of particle accelerators. The process used here draws on the similarities between the ways that the two mechanisms drive flow fields to supercritical velocities. In order to simplify the comparison process, the physics used to model the acceleration of the fluids in the flow field is simplified and does not properly take into account relativistic effects. Such a simplification brings about similarities between the two processes so that methods developed for sub- and supersonic flow fields may be applied to particle accelerators. The possible acceleration of streams of charged particles to critical and supercritical velocities is explored theoretically, but a connection between supercritical and relativistic velocities is not made.

The objective of this paper is to present the development of an acceleration method for charged-particle accelerators that are similar in some ways, but also different from the wind tunnel acceleration method. That is, instead of pressure forces in a neutral gas, the acceleration of charged particles is based on electrostatic forces to bring about the acceleration of the stream of charged particles. Wind tunnel design principles for a neutral gas like air are then theoretically adapted to produce analogous stream geometries that accelerate streams of charged particles to supercritical velocities. The analysis is then facilitated by development of flow-field models, their partial differential equations, and flow-field geometries that parallel those for wind tunnel

---

<sup>1</sup>Ames Associate, Aviation Systems Division, Ames Research Center, Mail Stop 210-10, Moffett Field, California 94035-1000.

airstreams, but which are adapted to streams of charged particles. It is found that the two analyses for the similar parts of the two flow fields have the same form when each is made dimensionless by use of their respective critical velocities.

The critical velocity of a compressible gas is defined as the velocity of propagation of a small-amplitude disturbance compression or expansion wave through the gas in the stream. In wind tunnels, the critical velocity is the same as the molecule-driven speed of sound. Because an expression for the critical velocity for a stream of charged particles could not be found in the literature, an expression for its formulation is derived in the Appendix of this paper. A derivation is also presented there for the wave velocity and for the equation of state for a stream of charged particles. These derivations make it possible to treat the flow fields of charged-particle accelerators with the same types of differential equations that are presently being successfully applied to the flow fields in supersonic wind tunnels and around supersonic aircraft.

Based on the derivations presented in the Appendix, the body of the paper presents an analysis of the characteristics of charged-particle flow-field channels needed to bring about the transition of the flow-field velocities from subcritical to supercritical. It is noted that the pressure forces in the flow field of supersonic flow fields are not stationary, but are designed to move with the aerodynamic elements of the stream. In contrast, streams of charged particles are presently usually driven by use of force fields that are fixed to a laboratory frame of reference, making acceleration of stream elements beyond supercritical stream velocities difficult. A discussion is then presented of the flow-field characteristics to be expected when flow fields composed of charged particles are driven by flow-field components that are flowing at velocities up to those greater than their critical velocity.

In order to illustrate possible ways to use the analogy, the well-known theoretical solutions for the structure of small-amplitude compression or expansion waves, called Mach waves, are derived for the supercritical flow of an electron gas for both Mach waves and for the supercritical flow around a sharp corner. The solutions illustrate that the development of other supercritical flow fields can also be accomplished for streams of electrons by use of the analogy described. As stated previously, the possible acceleration of streams of charged particles to critical and supercritical velocities is explored theoretically, but a connection between supercritical and relativistic velocities is not made.

## I. INTRODUCTION

Prior to the 1920s, it was believed that flight of aircraft could not be made at or above velocities at the speed of sound because the aerodynamic loads on the aircraft at or above the those velocities would destroy the aircraft. The impression was so prevalent that sonic velocity was labeled a sound barrier to the search for the achievement of flight velocities at and above the speed of sound. Unrestrictive research and development efforts during World War II produced not only theoretical tools for the design of missiles and aircraft that could safely fly at and above the speed of sound.

Comparable efforts that have been underway for some time to accelerate charged particles to velocities significantly above the speed of light have met with marginal success. For this reason, the present study was undertaken as an investigation based on the similarity of a portion of the flow fields of supersonic wind tunnels (refs. 1–17) to those of a portion of charged particle accelerators (refs. 17–20). The study as analogous flow fields is used to guide the search for a method that will increase the performance capabilities (e.g., increase velocities and efficiencies, and/or stream volumes) currently achievable with charged-particle accelerators.

It is first noted that the flow fields of supersonic wind tunnels (refs. 1, 2) and of charged particle accelerators (refs. 19, 20) are similar or analogous to each other mostly over the portion of their circuits that involve stream acceleration without power addition or removal. Therefore, the study presented applies to the non-powered and non-dissipating parts of both of these circuits because that is where the fluid-dynamic flow fields of the two devices have the similarities being studied in this paper. Those parts of the two flow fields are located where the flow-field geometry of each of the two streams should make the transition from a low sub-critical velocity up through their respective critical velocity to their designed supercritical velocity. Therefore, the flow-field regions chosen for this study are first defined for the flow fields of supersonic wind tunnels, partly because wind tunnel circuits are simpler in structure and partly because their design is more mature than the corresponding circuits of charged-particle accelerators. The information derived from the structure of supersonic wind tunnels is then used in Section VI to guide the theoretical design of charged particle accelerators that have the potential to achieve stream velocities that exceed their critical velocities. The design, like the one for wind tunnels, is based on the size of the cross-section of the stream boundaries as a function of distance along the channel to bring about supercritical velocities in the stream.

The purpose of the study reported is to explore theoretically whether it is possible, and if so, how best to use the information available on the two foregoing analogous flow fields in order to develop designs for charged-particle accelerators that will accomplish for particle velocities on a controlled and consistent basis a comparable technology that has long been available for aerodynamicists. It is recognized that the simplifications made in the analysis may result in the prediction of particle velocities greater than the speed of light in a vacuum relative to a laboratory frame of reference. However, enough similarities are shown between the two processes to indicate that there may be an application of methods developed for supersonic flows to particle accelerators. The objective of the study is to formulate experimental systems that are both more efficient and that bring about larger velocity magnitudes than are currently being achieved with the present designs of particle accelerators. In order to illustrate some advantages of the analogy, the well-known theoretical solution for the supersonic flow across Mach waves in air and around sharp corners, as developed in the early 1900s for the structure of Mach waves, is used here as a model for the derivation of similar flow fields that apply to the supercritical flow fields of streams of an electron gas. The flow-field concepts being explored are first treated as one-dimensional flow-field problems, and then as two or three dimensional flow fields; i.e., a Prandtl-Meyer expansion fan that applies to supercritical streams of charged particles.

This study begins with a brief discussion of the hardware used for the flow fields associated with subsonic and supersonic wind tunnels. The following section then provides a description of the parameters that will be used to identify and differentiate the various flow-field parameters that

will be used in the analysis to be presented. The sections that follow describe the differential equations associated with the two mediums (i.e., streams of neutral gases like air, and streams of charged-particle gases like a stream of electrons) along with how supercritical flow fields are achieved in each of the two flow-field types being considered in the analogy. In particular, the reasons why certain streamwise variations in the cross-sectional size of the flow-field channels for the two fluids are necessary if streams of charged particles are to be accelerated through a transition from subcritical to supercritical velocity. The paper presents an analysis of the characteristics of the two flow-field channels needed to bring about the transition of the flow-field velocities from subcritical to supercritical.

The presentation then turns to the premise that the analogy of the flow field of an electron gas is in many subcritical and supercritical ways similar to the corresponding flow fields of neutral gases like nitrogen, oxygen, and air. An important difference is the fact that the fluid dynamics of streams of electrons differ from streams of neutral gases studied here in that there are no random thermal motions of the gas particles in the electron gas. Therefore, even though the mechanisms that cause a gas of neutral particles to behave like a gas of charged particles is different, the aerodynamic characteristics of the stream of air and of the stream of electrons are, however, enough alike that solution methods developed for streams of neutral particles can also be applied to the analysis of, and the flow-field characteristics of, streams of electrons.

The foregoing observations indicate that many of the important idealized flow-field structures developed in the past for the aerospace industry (refs. 1–17) can also be reconstructed or adapted for use when streams of charged particles, like the streams of electrons, are being studied. Because a number of excellent texts have been written on the experimental and theoretical techniques for aerodynamic flow fields, several of the more important flow-field examples will be adapted to streams of electrons to illustrate how the power of well-known aerodynamic methods can be adapted to streams of charged particles like electrons.

The various books (refs. 3–15) listed as references present slightly different versions and results for the variety of flow fields that are common to aerodynamic problems associated with sub- and supersonic flow fields for a wide range of situations. Although most were prepared some time ago, they are still applicable and serve as useful information sources on the subject. Reference will most often be cited to the texts prepared by Liepmann and Puckett (ref. 12), Courant and Friedrichs (ref. 13), and the two volumes by Shapiro (refs. 14, 15). These texts contain a number of excellent illustrations of flow-field solutions and their derivations for air that help greatly to understand the solutions already developed and the range of possibilities available for possible adaptation from aerodynamic to electron streams. The references also provide excellent figures and explanations on the wide variety of solutions for supersonic flow fields that may help the reader to better comprehend and utilize the process of solution-development for the flow fields of charged particles. Because the derivations of suggested flow fields are often lengthy and complex, only a few of the illustrations of the structures of sample flow fields are presented to indicate possibilities. The texts and illustrations presented are intended to serve as a brief introductory discussion on some of the flow-field solutions that are common to both the flow of neutral gases like air and the corresponding flow-field structures of charged-particle gases like streams of an electron gas.

The information presented in this paper has application to charged-particle thrusters for use on space vehicles and to particle accelerators being used to study particle physics. The presentation does not, however, have application to the dynamics of ionized gases wherein both positively and negatively charged particles are present in charged-particle streams like the solar wind.

## II. EXAMPLES OF A SUBSONIC AND A SUPERSONIC WIND TUNNEL

In case the reader is unfamiliar with wind tunnel designs, several texts (refs. 1, 2) present information on the characteristics of a large number of both subsonic and supersonic wind tunnels. Figure 1 presents a sketch of the basic structure of a subsonic wind tunnel (ref. 2), and figure 2 presents a sketch of the basic structure of a supersonic wind tunnel (ref. 2). Two examples were chosen because they appear to be among the simplest available of a subsonic and supersonic wind tunnel, and appear to clearly show the parts that are essential for operation of each facility.

The schematic diagram of the subsonic wind tunnel shown in figure 1 illustrates how the stream of air enters the circuit of the wind tunnel, and how it is then guided by use of rounded inlet surfaces and anti-turbulence screens to smoothen the airstream into a uniform stream before it is concentrated and accelerated through a constant-area "test section" where experiments are conducted. The flow field in the test section is where the stream is nearly uniform and non-turbulent so that it simulates flight through the atmosphere, much like the ones that an aircraft

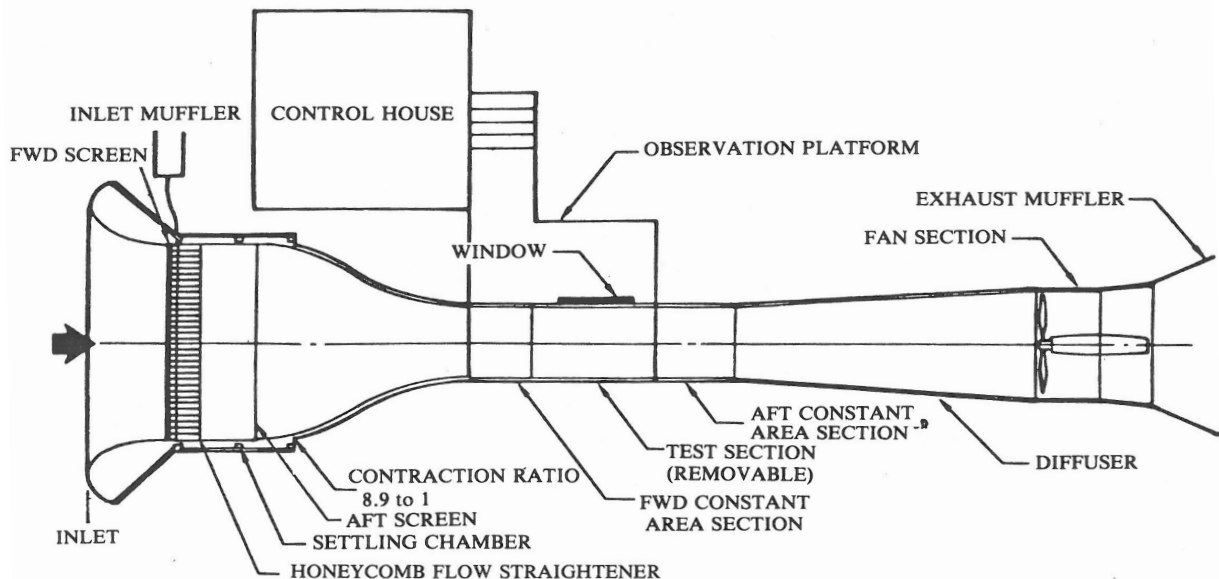


Figure 1. Schematic diagram of Boeing Commercial Airplane Co.'s open-circuit non-return flow-through subsonic wind tunnel; test section is 9 feet by 9 feet in cross section and 14.5 feet in length. Reproduced from Penaranda and Freda (ref. 2), p. 111A. The facility is a flow-through device and does not have a flow-return part.

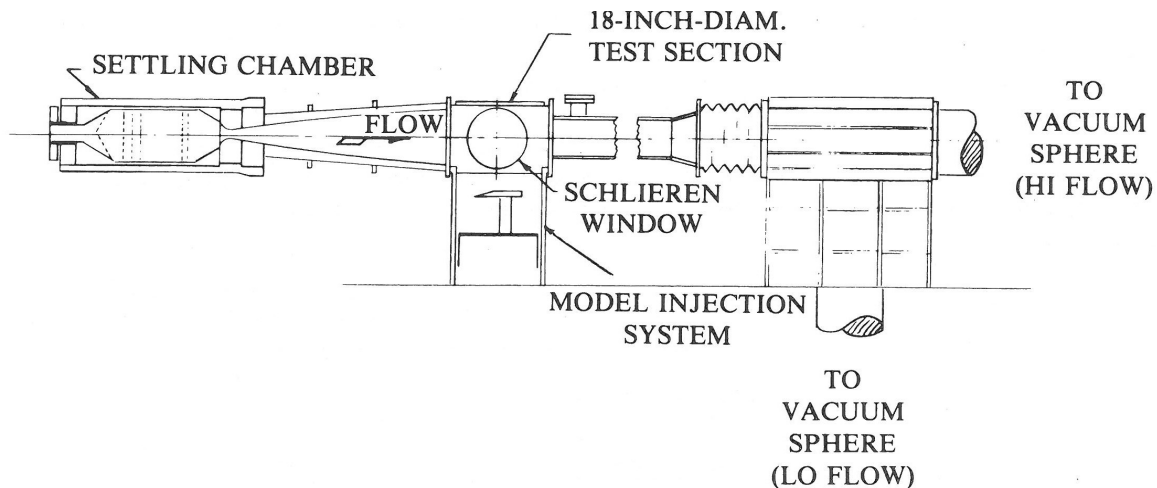


Figure 2. Schematic diagram of NASA Langley Research Center's Mach number 8 open-circuit non-return flow-through hypersonic wind tunnel. Test section is 18 inches in diameter and the usable diameter of the test stream is 4 to 14 inches in diameter depending on the pressure in the vacuum spheres at the time. Maximum run time = 1.5 min. Facility has a large amount of pumping and air-conditioning machinery that is not shown here. These important and mostly concrete and steel components are not shown because they do not require a unique design. (Penaranda and Freda, ref. 2, p. 269A.)

might encounter during flight. In this facility a fan or multi-bladed propeller located near the exit of the stream is used to pull in and drive the airstream at velocities comparable with those used for landing and takeoff operations of aircraft. The test section then acts like a minimum cross-sectional constraint on the flow field of a stream of air to produce a region in the facility where wind tunnel tests of aircraft, or one of their components, may be safely tested in atmospheric situations where the flow field is uniform to a high degree of accuracy; for example, to within about 1% of the maximum velocity. After the air passes through the test section, it is returned to the atmosphere in a direction away from the entry to the facility.

Figure 2 presents the flow field inside of a channel shown as an example of a supersonic wind tunnel. As with the design of subsonic wind tunnels, the channels used for supersonic wind tunnels also have the first part of their circuits devoted to anti-turbulence screens and to air-flow straighteners (not shown in figure 2) to condition the stream of air for acceleration to a supersonic velocity—which is 8 times the speed of sound in the airstream of this facility. In order to achieve such a velocity, the flow-field channel shown contains the added presence of a short, smoothly contoured minimum section or “throat” where the airstream passes through the speed of sound as it enters an expanding segment of the circuit or channel. The special shape for the interior of the channel, where a constriction is used to bring about a “throat” feature in the circuit of the wind tunnel, separates the upstream subsonic part of the circuit from the downstream supersonic part of the circuit that flows into the test section part of the circuit where aerodynamic data is obtained. The particular shapes for these parts of the channel flow field have been found both theoretically and experimentally to be necessary, if the stream velocity,  $U$ , is to make a transition from subsonic (or subcritical) to supersonic (or supercritical) flow velocities.

In supersonic wind tunnels, the critical velocity of the stream occurs at the station of minimum cross section in the channel where the Mach number,  $U/a$ , of the stream is equal to 1.0. If the proper pressure differences are imposed at the upstream and downstream ends of the channel, the stream velocity will make the transition from a subsonic (or subcritical) to a supersonic (or supercritical) velocity. This special shape for that portion of the wind tunnel channel provides an end to the subsonic region at the smallest or throat region of the shaped part of the channel. An end to the subsonic part, which is also the beginning of the test section part of the channel, is known as the supersonic part because of the specially shaped expanding part of the nozzle.

The sketch in figure 2 does not include the devices needed to compress and condition (i.e., remove dust particles and excess water from) the airstream for the beginning of its acceleration to supercritical velocities in the nozzle and the test section of the wind tunnel. The special design of the shape of the nozzle is described in refs. 12–15. The pumping equipment and vacuum spheres necessary for the downstream operation of the facility are not shown. For most of the purposes of the presentation in this paper, such an omission is permissible because the segments of the facility being chosen for the analogy are the nozzle and the test section regions. It is important, however, to bear in mind that the facility will not work without these additional and necessary parts of wind tunnel circuits. These entry, exit, and stream-return segments of the facilities are not unique in design. They are usually constructed of steel, and may vary considerably from one facility to the next. It is, however, the details of the interior shape of the contraction section, of the nozzle, and of the entry into the test section, that are of primary interest for the study of the analogy being considered here.

### **III. NOISE PROPAGATION PATTERNS FOR SEVERAL VELOCITY REGIMES OF MOVING DISTURBANCES**

#### **A. Critical Velocity and Mach Number**

As mentioned in the previous section, the critical velocity of a compressible gas is defined as the velocity of propagation of a small-disturbance compression or expansion wave relative to the gas, whether the gas is stationary or flowing in a stream. In this section of the paper, illustrations are first used to show how the almost continuous sequence of waves shed as aerodynamic noise from an aircraft and its engines (its acoustic signature) illustrate when and where information from it, as a moving noise source, is located as a function of time. In order to study this observational problem, it is assumed that as an aircraft moves through the atmosphere at a constant velocity, it emits a series of idealized small-amplitude disturbance waves that occur at regular intervals of time (e.g., a fraction of a second) during its flight. As shown in figure 3, the noise patterns shown are similar to those used by Mach and others (refs. 11, 14) to describe the several velocity and sound domains associated with aircraft or projectiles as they fly through the atmosphere at various Mach numbers. See reference 16 for a discussion of how Ernst Mach's name became associated with the velocity parameter  $V/a$ , where the parameter 'V' is the velocity of the vehicle (the noise source), and 'a' is the velocity of propagation of a small amplitude disturbance wave, or an acoustic or noise wave, through the gas. The ratio of the two parameters, velocity and speed of sound, are now well known to aerodynamicists as the Mach number of an

object moving through stationary air, or of a stationary object with a stream flowing past an observer at a given Mach number. It is assumed, as shown in figure 3, that the velocity of the noise source is given by the velocity “V”, and that “a” is the velocity of propagation of sound through stationary air, so that the Mach number is given by  $M = V/a$ . A wave front, if there is one, is present when the Mach number of the noise source relative to the atmosphere is greater than one so that the angle,  $\alpha$ , of the wave front relative to the direction of the stream velocity is given by  $\sin \alpha = a / V$ .

The discussion in this part of the paper notes that the observations made of an aircraft flight (the noise source) can be carried out by means of two methods: first by use of the speed of light (an optical signal that propagates at about  $3 \times 10^8$  meters/sec, by use of our eyes) and secondly by the use of the speed of sound (an acoustic disturbance or signal that travels at about 300 meters/sec (1,100 ft/sec) and may be detected by use of our ears). Such an assumption calls attention to the fact that the observations made of flying aircraft have both an acoustic and an optical signature. In most cases, the visual method is rapid enough so that it can be used to adjust or correct the acoustic location to obtain “significantly more accurate” measurements of the location and velocity of objects like aircraft through a medium such as air.

## **B. Velocity Domains of a Moving Noise Source Relative to Earth’s Atmosphere**

As mentioned in the previous section, the critical velocity of a compressible gas is defined as the velocity of propagation (relative to the gas, air) of a small-amplitude disturbance compression or expansion wave (ref. 12). It is also pointed out, that in gases like air, the critical velocity and the speed of sound are the same. Because the wave speed in air is molecularly driven, the speed of sound is derived from the equation of state as

$$dp/d\rho = \gamma p/\rho = \gamma RT = a^2 \quad (1a)$$

or

$$a = (\gamma RT)^{1/2} \quad (1b)$$

The parameter,  $\gamma$ , is the ratio of the specific heat of air at constant pressure, to the specific heat at constant volume so that  $\gamma = C_p/C_v$  (theoretically estimated at 1.4, and measured at 1.405, and the gas constant parameter, R, has been determined as  $1715 \text{ ft}^2/\text{sec}^2 \text{ } ^\circ\text{F}$ , in English units). It is pointed out that, for a gas like air, the theoretical and the measured speed of sound are found to be a function of only one parameter, the absolute temperature, T, of the gas, which is a measure of the average velocity of the molecular motions in the gas.

The discussion in this section first assumes that the observations made of the flight of an aircraft, and its noise (or acoustic) and movement patterns, can be carried out by means of two methods. The first method uses the speed of light (as part of a sensor method that monitors movement by use of light waves, which have a sensing velocity of about  $3 \times 10^8$  meters/sec), or with a visual-based method (e.g., our eyes) that monitors movement by sensing the location of an aircraft as a

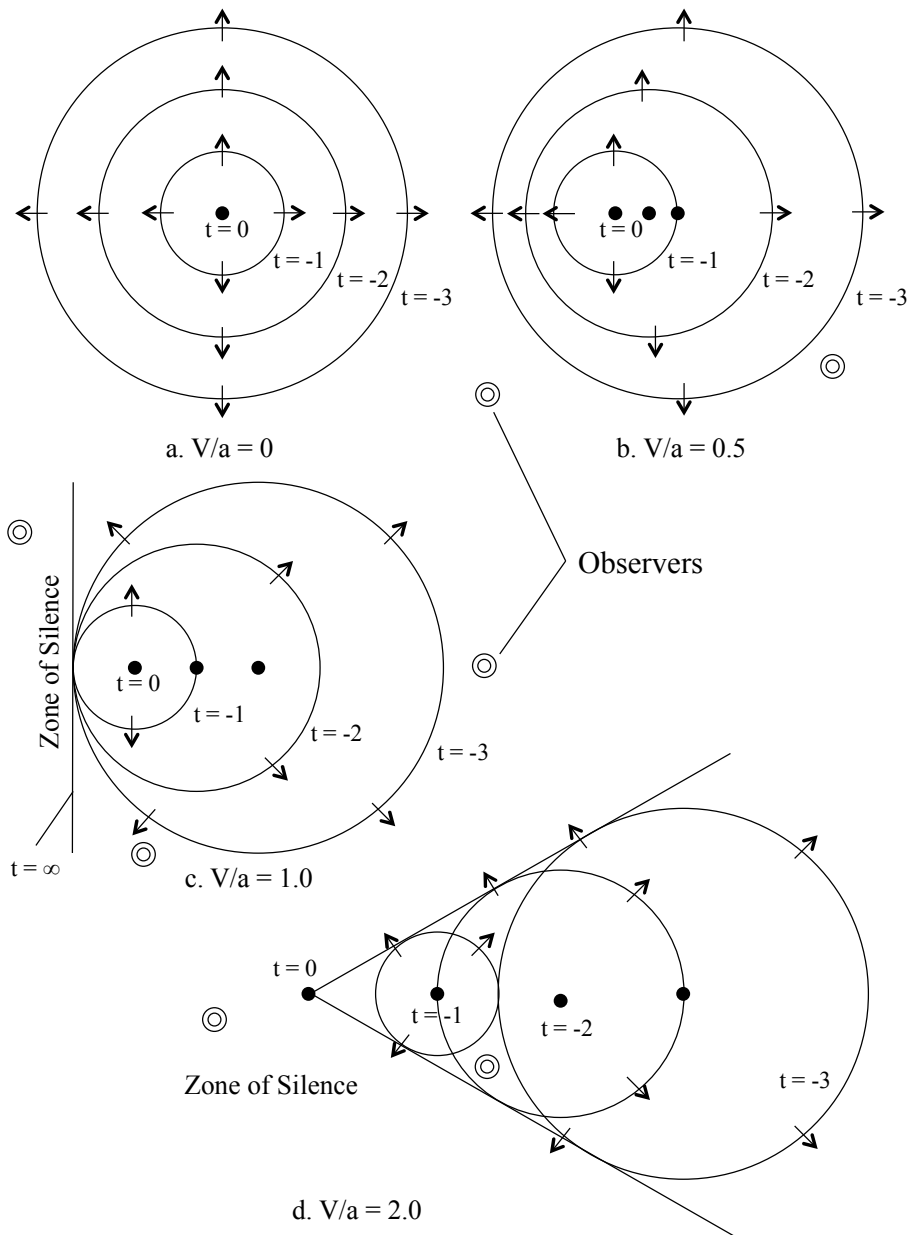


Figure 3. Illustrations of patterns of sound waves as a function of time as generated by an object or aircraft as it flies through a gas like air at four different velocities. The quantity 'a' in the figure captions denotes the critical velocity of the gas through which the object is flying (in this figure, as for neutral gases, the critical velocity and the speed of sound, a, are the same) and the quantity 'V' denotes the velocity of the object relative to that of the gas, which is assumed to be stationary in the present examples.

function of time. The second method makes use of sound-based (acoustical) sensing equipment (e.g., our ears) where the observation velocity is about 305 meters/sec (1100 ft/sec). That is, visual locations are theoretically about  $10^5$  times more rapid (and more accurate) in both location and time than are acoustic methods. This fact calls attention to the fact that the observations

made of acoustic events by use of visual methods can be used to correct or interpret observations, or measurements, made in order to obtain “significantly accurate” measurements of the velocity and location of objects like aircraft as a function of time. However, the velocity and location of rapidly moving small objects like charged particles through mediums like air or through empty space (like vacuums) must, because of their high velocities, usually be carried out only by use of optical methods.

In order to set up experiments that probe the physics of aircraft- and particle-velocities, and their measurement, the noise-generation (or acoustic) patterns and their propagation with time are now discussed in order to achieve an improved understanding of how observation methods must be carried out in order to avoid the production of misleading interpretations. The study first considers the four idealized patterns presented in figure 3 as acoustic or noise patterns. They illustrate idealized noise patterns for one stationary (fig. 3a) and three moving (figs. 3b, 3c, and 3d) aircraft noise patterns. The circular lines in the four parts of figure 3 represent time-wise locations of periodic sound waves that are shed by a single moving noise source, like the jet engine of an aircraft. The four cases illustrate and identify the four velocity regimes that include one stationary noise source and three noise sources that are moving at velocities that include a fraction of the speed of sound, the speed of sound, and two times the speed of sound.

Because the speed of sound in a gas like air is the same as its critical velocity, the discussions to follow will use the expressions ‘critical velocity’ and ‘speed of sound’ interchangeably. For example, the four illustrations in figure 3 represent situations where an aircraft is assumed to generate a noise pulse at regular intervals of time or distance (because the vehicle is assumed to be moving at a constant velocity). The velocity of the source that is generating the noise patterns in the four parts of figure 3 are assumed to be stationary, subcritical, critical and supercritical in that order. (It is noted that the same reference velocities used for situations in the atmosphere also apply to the flow fields in wind tunnel circuits, if the frame of reference is changed.) The four figures shown in figure 3 represent the wave sizes and their locations relative to the location of the aircraft at a given time. That is, it is assumed that the velocity of each of the noise sources is moving at a speed that is stationary in figure 3a, at 0.5 times the speed of sound in figure 3b, at the speed of sound in figure 3c, and at two times the speed of sound in air in figure 3d. Of course, it is assumed in all of the parts of figure 3 that the wind velocity is negligible and that the flight velocity is constant in magnitude and direction during the part of the event that is being observed.

The speed ratios,  $V/a$ , in the four figures shown are now known as the Mach numbers (ref. 16) of the aircraft or of the object that is generating the acoustic signatures being illustrated. The same velocity concepts shown in figure 3 also apply to wind tunnels, and have sometimes resulted in the naming of facilities according to their Mach number capabilities (e.g., figure 1 presents a facility that can operate over a range of subsonic Mach numbers, and figure 2 illustrates a facility that operates at only the one Mach number,  $M_a$ , which is 8 for that facility).

In figure 3a, where the aircraft is assumed to be stationary, the periodic sound waves (circular lines) are all concentric circles because, in the uniform atmosphere assumed here, all of the sound waves originated at the same location, and at regular intervals of time, so that the

appearance of the sound waves are concentric circles. Therefore, as the disturbances age, the diameters of the circles they produce increase linearly with time as the parts of the various waves propagate through the uniform and stationary atmosphere. The wave pattern shown in figure 3a is then a set of concentric circles, where the oldest disturbance is the largest circle and the smallest is the one most recently generated. An observer located on any side of the noise diagram in figure 3a then hears the engine noise at its location without distortion or change of frequency.

When the noise-generating aircraft is moving (e.g., at half or 0.5 times the speed of sound), it is moving at what is referred to as a subcritical wave velocity (or Mach number of 0.5 ( $M_a = V/a = 0.5$ )). Each of the three circular waves shown in figure 3b then have the same size and shape as in figure 3a, but the waves are now displaced relative to each other, because the noise source has moved between the generation of each noise wave. An observer off to the side of the pattern recognizes the offset of the circles as motion of the generating aircraft. As is often the case, on hearing the noise from a subsonic aircraft, the observer knows from previous experiences that the visual image of the aircraft does not come directly from a stationary source where the noise is being emitted, but must look for the aircraft somewhere ahead of where the sound pulse originated. The observer also learns by experience that aircraft flying at larger velocities have a greater distance between the visual- and sound-determined, or sound-identified images, and that there is usually only one center of noise generation and one of visual center.

When the velocity of the aircraft is increased to  $M_a = V/a = 1.0$ , as shown in figure 3c, the velocity of the aircraft is moving at the same velocity as the critical wave velocity, or the speed of sound, of the air at that location. The circular wave patterns for the three instances of time are again the same three sizes, and are not distorted in shape, but are displaced relative to each other just enough that the circular waves are all coincident on the front part of their crests as indicated in figure 3c. However, the separation distance between the centers of noise and the visual centers are now larger and more confusing. First, because the waves are all coincident on the front side of the wave pattern, an observer located ahead of the aircraft will visually “see the aircraft” but does not “hear” the noise generated by the aircraft until the aircraft has passed the observer, thereby creating a “zone of silence” at any location ahead of the aircraft. At the moment that the concentrated wave front passes, the observer hears an unusually loud and sharp bang. After the aircraft and its waves pass the location of the observer, the amplitude of the sound decreases due to distance and to dissipation of wave energy with time and distance. On the front side of the wave pattern, only one center of the noise source appears to exist, and it appears to have an almost explosive front side. However, after aircraft passage, the noise sources appear to be continuously coming from behind AND along the approach flight path of the aircraft, and its frequency appears to be variable. For this reason, the noise patterns observed give the impression that a second aircraft is behind the first one and flying in the opposite direction. Of course, although it appears that the aircraft is being heard at a given location, the aircraft is actually elsewhere making those sound pulses at a “significantly displaced” sound-image location of the real flow field.

When the velocity of the aircraft is increased to twice the speed of sound, or  $M = V/a = 2.0$ , figure 3d, the velocity of the aircraft is twice that of its critical wave velocity, or the speed of sound. The displacements of the circular waves between each time interval are now so large that the waves are all coincident on a front part of their crests as indicated in figure 3d, to produce a slanting wedge-shaped wave front. The location of the aircraft is now at the point of the wedge-shaped wave front, no matter what the observing time. A zone of silence is now located not only directly in front of the aircraft, but also in regions above and below the ever-broadening wedge-shaped wave pattern shown in figure 3d. Each circular acoustic wave is again not appreciably altered, but the arrival of each sound wave at a given location, as a function of time, is quite different. For example, the first noise heard by the observer shown in figure 3d, after having just entered the noise region generated by the aircraft, is the loud bang of the arriving concentrated (or shock) wave and also a series of sound pulse that originated a little more than one time interval after passage of the aircraft. In addition, the observer also hears what sounds like the passage of another aircraft that has sound waves that seem to have originated about two pulses earlier than aircraft passage. Observation of these two sound pulses at about the same time, even though they were originated at a long distance (and a long time) apart, suggests that supersonic flight produces one real noise or acoustic source, that is traveling in the same direction as the aircraft, and a second sound or acoustic source (a non-real or ghost image) that is associated with noise pulses produced much earlier in the flight history of the aircraft. Also, the second sound image of the non-existing noise source appears to be travelling away from the observer (and in the opposite direction of the actual aircraft flight direction). It then appears acoustically to the observer that the second (and non-real) sound image is moving in a direction opposite to that of the wave-generating aircraft!

It is to be noted by the observer, that two sets of sound images arrive (at an observer) in both the order generated and in an inverse order depending on the time when generated, and on the relative locations of the observer. That is, the time-wise sound images produced by the event and received by an observer will be partly in the same order and partly in an inverse order. For this reason, although the false sound image contains the same sound or acoustic information as the original image, the information in the second (or false) image arrives in a reverse order that sounds somewhat like the original and somewhat scrambled.

When the phenomena is observed in person, the observer is first tempted to conclude that two aircraft have flown past his station, one in each of the two directions aligned with the flight path of the aircraft; one noise source sounds as it should, and the other sounds non-real—and sounds as if it is flying away from the observer. More detailed study (and longer periods of observation) indicate that the apparent motion of the older and “retreating acoustic image” should not be associated with the observed time of the noise, but with the “corresponding adjusted arrival times of the various noise pulses.” The diagrams presented in figure 3 indicate that “false” sound images only occur when the noise source (usually an aircraft) is moving at velocities equal to or greater than the speed of sound (which are labeled as at supersonic or supercritical velocities). Observations of aircraft making a series of low-altitude high-speed research flights over runways at research stations prompted and support the time- and direction-based descriptions reported here.

### C. Velocity Domains of Moving Electromagnetic Noise Source in Atmosphere of Charged Particles Like Electrons

The rules for the structure and the dynamics of an electron gas are presented in the Appendix to establish the rules for the location and timing of light or optical noise sources being generated in figure 3. In many respects the optical wave phenomena are similar to the corresponding acoustic ones discussed previously. However, observations now become more difficult because the observations can now only be made with electromagnetic or optical tools; that is, the use of sound waves as a second monitoring method is impractical because the propagation velocity of acoustic waves is far too small in comparison with the speed of the propagation velocity of electromagnetic waves (e.g., sound travels more slowly than light waves by a factor of about  $10^5$ ).

Even so, the foregoing acoustic observations still suggest that similar “ghost” images might also be observed in experiments where charged particles pass through a stationary target material at velocities larger than the speed of light in that medium (ref. 20). If true, it is suggested that the particle paths visually observed in the various experiments might have been displayed by one real and one “false” or “ghost” image of the incident particle, as described in the foregoing text for the similar “acoustic” experiment. If so, a second particle may again appear as a non-real source as indicated by the foregoing acoustic experiment, rather than a second or new particle. Because the sequence in which the light pulses arrive at an observer will usually be partly in sequence and partly in an inverted sequence, an overall image of a second (perhaps false) particle will be difficult to discern without careful analysis of each event. The apparent motion of a second or “ghost” “optical-noise” source may (as in the acoustic-noise experiment) be entirely or closely related to a partially or completely “inverted” image of the original particle, if the optical and acoustic experimental situations being produced are indeed similar.

## IV. EQUATION OF STATE AND CRITICAL SPEED

### A. Streams of Air

In discussions to follow, the parameters,  $\rho$ , as density,  $p$ , as pressure,  $T$ , as temperature and,  $g$ , as the acceleration of gravity, are used in the aerodynamic sense in that the presence of, or bombardment on a surface by, a large number of very small particles (like air molecules) are added together to form the pressure in a gas or on a given surface and/or the density of a gas. That is, the action of an assembly of particles, whether charged or neutral, to produce a given force per unit area or to produce a given mass per unit volume will be used in what follows to study flow fields in both the aerodynamic and electrodynamic sense. As stated previously, because sound waves are small amplitude compression or expansion waves, their velocity of propagation (e.g., through air) is the same as the speed of sound. The speed of sound in air can be expressed in various thermodynamic ways by use of the equation of state for gases (ref. 10), which is written here as

$$p_a = \rho_a R_g T_a \quad (1)$$

where the subscript, a, is used to denote that it is for an atmospheric parameter, or for air. The parameter,  $p_a$ , is then the pressure, and  $\rho_a$  is the density of the gas, the quantity  $R_g = 1715 \text{ ft}^2/\text{sec}^2 \text{ } ^\circ\text{F}$  is the universal gas constant in engineering nomenclature for neutral gases, and  $T_a$  is the absolute temperature of the gas/air in degrees Rankine.

Now consider a gas composed entirely of charged particles like electrons, all equally spaced at a distance,  $d_e$ , as described in the Appendix to this paper. The various properties of such a gas are then estimated (see Appendix) as

$$\text{density} = \rho_e = m_e(1/d_e)^3 \quad (\text{A3a})$$

$$\text{pressure} = p_e = (e^2/4\pi K_0)[1/(d_e^2)] \quad (\text{A3b})$$

so that,  $a_e^2 = dp_e/d\rho_e$ , for the flow-field model assumed,

$$a_e^2 = (e^2/4\pi K_0 m_e d_e^2) \quad (\text{A15})$$

or

$$a_e = (e^2/4\pi K_0 m_e)^{1/2}/d_e \quad (\text{A16})$$

When the numerical values for the various constants in Eq. (A16) are substituted, the expression becomes,

$$a_e = 25.33/d_e \text{ m/sec} \quad (2)$$

Because the working fluid/atmosphere is now composed of electrons, rather than air molecules, the various parameters associated with the “electron gas” being used are each identified by use of a subscript “e.” The “speed of sound” in such a gas is then inversely proportional to the spacing between electron centers, and not to the temperature of the gas, which is assumed to be zero. That is, the more dense (the smaller the value of  $d_e$ ) that the electron gas becomes, the higher the critical velocity,  $a_e$ . The non-linear ( $d_e^2$ ) repulsion force that exists between the electrons in this model of an electron gas determines the value of  $a_e$ . the velocity of propagation of a small amplitude compression or expansion wave through an electron gas.

It is also assumed that the energy contained in any random motions in the electron streams is negligible in comparison with the energy contained in the bulk motions of any organized motion of the velocities of the electrons. The kinetic energy in the reservoir, or in stationary parts of the electron gas, are then zero, so that all of the flow fields to be studied may be treated as at a zero molecular, or particle temperature, so that they may, and will, be left out of the analogy being used.

In the present text, the parameter,  $\gamma_a$ , is the ratio of the specific heat for air at constant pressure,  $C_p$ , to the specific heat for air at constant volume,  $C_v$ , as,

$$\gamma_a = C_p/C_v = (N + 2)/N \quad (3)$$

The parameter  $N$  is the number of degrees of freedom for the particles of gas that make up the stream being used. For example, if  $N = 3$ , as for mono-atomic gases,  $\gamma = 1.6667$  because single atom molecules have only the three directions of travel that yield significant energy for their degrees of freedom. For diatomic gases, like oxygen and nitrogen, the ratio of specific heats is calculated with the parameter  $N = 5$ , because the molecules have significant energy content in the three directions of travel, and also in the two modes of rotation that contribute significantly to the energy of the gas. In those cases, the degrees of freedom for those gases are  $N = 5$  so that  $\gamma_a = 1.4$  for diatomic gases. Because air is a mixture of mono-atomic and diatomic gases, the experimental, and more appropriate, value for  $\gamma_a$  is actually about 1.405 (ref. 12). In this way, the speed of sound in a gas composed of only electrically neutral particles is a function only of the temperature (as represented by the velocity of motion and of rotation of the particles) of the gas as given by Eq. (2). That is, the temperature of the gas represents an average velocity of the molecules of the gas, which is the parameter that passes information from one layer of fluid to another. In stationary or moving bodies of air at room temperature, the speed of sound is somewhere around 1,100 ft/sec ( $\approx 335$  m/s) relative to the motion of the fluid.

In most gas-dynamic flow fields, it is assumed that the compressibility of the medium (air in this case) is the characteristic that participates in the wave-producing process, and that the compressibility is brought about by the thermal motion of the particles that make up the gas (air in most cases). It is also generally assumed that the wave travelling at the speed of sound transfers momentum but no heat or thermal energy from one layer of the fluid to the next (i.e., fluid motions are carried out adiabatically). That is, pressure information and density changes are passed quickly from one layer of fluid to the next, but heat transfer is a much slower process and will generally be ignored in the present discussion. The speed of sound given by Eq. (A16) then divides the velocity of a flow field into two groups. That is, if the fluid velocity along a channel is smaller than its speed of sound, the flow velocity is referred to as being subcritical or subsonic, ( $u < a_a$ ), and if the fluid velocity along a channel is greater than the speed of sound, the flow velocity is referred to as being supercritical or supersonic, ( $u > a_a$ ). If the fluid velocity is near its speed of sound, it is often referred to as being at or near its critical velocity, or as a trans-sonic flow field where  $u_a \approx a_a$ .

The parameters and the combinations of wave velocities used in this paper require that proper choices be made for the nomenclature used in each of the two analogous flow fields. As a reminder, the symbol for the velocity of propagation of a small disturbance compression or expansion wave through a stream of molecules of air is usually expressed as both its critical speed and its speed of sound. As discussed in the previous section, the reference velocity commonly used in wind tunnel streams is the speed of sound of the stream of gas, and it is

usually denoted by the letter ‘a’. In this paper, the letter ‘a’ will be used as the symbol for the speed of sound and also as a subscript to parameters in order to designate the fact that the given parameter applies only to air. For example, the symbol ‘ $a_a$ ’ is the speed of sound parameter only for air.

The corresponding reference velocity for streams of charged particles is derived in the Appendix and is again designated by the letter ‘a’ but with the letter ‘e’ as subscript to designate the parameter,  $a_e$ , as the corresponding quantity for the speed of sound in or the critical velocity for streams of electrons. As such, both symbols represent the velocity of propagation of a small disturbance compression or expansion wave through a stream of molecules of air, or of electrons, as the case may be. Such an arrangement facilitates any discussion of the analogy because, even though the velocities of a stream of air are on the order of the speed of sound in air (usually about 335 m/s (1,100 ft/s)), and the corresponding parameter for a stream of electrons, (which is usually a large fraction of the speed of light ( $2.998 \times 10^8$  m/s, but not the speed of light), is about five orders of magnitude larger than the speed of sound in air. The difficulties associated with such large differences in the sizes of these two reference velocities disappears when the propagation velocity for each flow field is written in dimensionless form by use of its own propagation velocity of disturbance waves for each medium; namely ‘ $a_a$ ’ and ‘ $a_e$ ’.

As will be seen in the remainder of this paper, the parameter ‘ $a_e$ ’ is not the speed of light,  $c$ , but, at this time, may be equal to, or smaller than or larger than the speed of light  $c$ . For this reason, velocity ratios are formed in each of the two analogous flow fields (one composed of air molecules referenced to ‘ $a_a$ ’, the speed of sound in air, or its critical speed) and the other, composed of electrons, is referenced to the corresponding critical speed parameter in an electron gas, ‘ $a_e$ ’, and not the speed of light. The use of these two speeds of propagation facilitates comparisons and the formation of similarities.

As mentioned previously, the first and most common velocity ratio to be used in the analyses to follow is based on the conventional Mach number that is regularly used in wind tunnels and in studies that are aerodynamic in character (ref. 16). The second most often Mach number ratio to be used in the present study applies to streams of electrons and is identified as  $M_e = U_\infty/a_e$ . The subscript ‘e’ denotes that the particles in the stream are electrons, and  $a_e$  designates that the reference (or critical) velocity is based on the velocity of propagation of a small compression or expansion wave through an electron gas (see Appendix A). A third velocity-based parameter is identified as the ratio of the velocity in any type of stream to the velocity of light,  $c$ , which may be written as  $M_c = U/c$ .

## **B. Stream of Electron Gas**

It is well known that the critical velocity of a neutral gas, like air, is the speed of sound in the stream. In flow fields of streams of charged particles, the velocity of propagation of a small

amplitude disturbance wave is, in this paper, associated with the electrostatic forces of repulsion between the charged particles (electrons) in the stream. As stated previously, because a theoretical expression for the velocity of propagation of a small-disturbance compression or expansion wave could not be found in the literature, an expression for its formulation is derived in the Appendix of this paper along with its equation of state and speed of sound for an electron gas. In the derivation, it is argued that relativistic corrections between streamwise layers of electrons are not needed because the relative velocity differences between any two nearby layers of electrons that drive disturbance waves, the difference in their velocity (or their relative velocity) is negligible in comparison the speed of light. The derivation of the wave velocity and the equation of state for the gas in a stream of charged particles are presented there to make it possible to treat the flow fields of charged-particle accelerators with the same type of analysis that has already been successfully derived and applied to the flow fields of supersonic wind tunnels. The derivations in the Appendix thereby make it possible to establish an analogy between the two flow fields being discussed here. The part of each of these two flow-field circuits that were chosen for study are treated as similar because both streams are able to respond as compressible fluids with known relationships for the efficient and robust wave dynamics that occurs in flow-field types of situations.

Because it is assumed that the pressure-density relationship is based on the assumption that no significant random thermal motions are present in the electron gas being studied, the equation of state depends only on the force field of the electrons on each other. The equation of state for a “cold” electron gas then depends only on the density of the electron gas,  $\rho_e$ , and the pressure,  $p_e$ , in the gas brought about by the forces of repulsion between the electrons in the gas. The equation of state for an electron gas may therefore be represented by a combination of Eqs. (A12) and (A14) presented in the Appendix of this paper as

$$\rho_e = m_e / (d_c)^3 \quad (4a)$$

$$p_e = (e/4\pi K_0 d_c)^2 = (e/4\pi K_0)^2 (1/d_c)^2 \quad (4b)$$

where the quantity,  $d_c$ , is the separation distance between centers of electrons. From Eq. (A12), the distance between electron centers is denoted by the parameter,  $d_c$ , and the density of the gas is given by

$$1/d_c^2 = (\rho_e/m_e)^{2/3} \quad (4c)$$

because the electrons are assumed to be centered on a rectangular mesh. Eq. (A14) may then be written as an equation of state relationship for an electron gas as

$$p_e = [e^2/(4\pi K_0)^2][(\rho_e/m_e)^{2/3}] \quad (4d)$$

When numbers are inserted into Eq. (4b), it may be written as

$$p_e = \rho_e^{2/3} [e^2/(4\pi K_0 m_e^{1/3})^2] = C_e \times \rho_e^{2/3} \quad (4e)$$

$$\begin{aligned}
\text{where, } C_e &= (1.60207)^{+2} (10^{-38}) (8.988)^{+2} (10^{+18}) (9.11)^{-2/3} (10^{+20+2/3}) \\
&= (2.5666283)(80.784)(94.36193)(0.229256)(4.64158) \\
&= 2.0820 \times 10^{+4}
\end{aligned}$$

In the foregoing equations, the pressure,  $p_e$ , is in  $\text{kg/m}^2$  and  $\rho_e$  is in  $\text{kg/m}^3$ . The equation of state for the idealized electron gas being explored here then becomes

$$p_e = \rho_e^{2/3} [e^2 / (4\pi K_0 m_e^{1/3})^2] = 20820.0 \rho_e^{2/3} \quad (4f)$$

or

$$p_e / \rho_e^{2/3} = \text{Constant} = 20820.0 \quad (4g)$$

The speed of a small disturbance wave through an electron gas is then given by an expression discussed previously as

$$a_e = (dp_e / d\rho_e)^{1/2} \approx (e/d_e) / (4\pi K_0 m_e)^{1/2} \quad (4h)$$

The quantities derived for the speed of sound parameter (i.e., the speed of propagation of a small disturbance compression or expansion wave) turn out to not be the speed of light, but one that parallels the “speed of sound” or the critical velocity parameter commonly used for streams of air in wind tunnel channels.

As a reminder, in magnitude, the speed of sound parameter used in streams of charged particles is on the order of magnitude of the speed of light, but it is not based on, or related to, the speed of light in a vacuum. That is, the reference velocity parameter for streams of charged particles is, like that of air, based on the velocity of propagation of a small compression or expansion disturbance wave through the test medium. In other words, the parameter represents the transmission of pressure and velocity (but not of light nor heat energy) information throughout the flow field being studied. In this paper, transmission of heat by conduction is assumed to be slow enough, compared with particle velocities, so that it is negligible in comparison with possible convective transmissions. Mixing of particle species are ruled out because both of the flow fields being studied in the analogy are assumed to be homogeneous. It is also assumed that the influence of light waves on the flow-field dynamics is negligible in comparison with the pressure and velocity energy forms of momentum and energy, and that pressure waves are transmitted by ‘sound’ or small-amplitude pressure waves at the critical velocity of whichever ‘gas’ is being used.

As noted in Eq. (4h), the speed of sound parameter for an electron gas uses the letter ‘e’ as a subscript and as the electronic charge on an electron in Coulombs for the quantity,  $m_e$ , with the mass of an electron in kg. As stated previously, the subscript ‘e’ denotes that the parameter to which it is attached designates that the parameter is for electrons. For example,  $d_e$  is the undisturbed distance between electron centers in the fluid in meters. The parameter,  $K_0 = 8.988 \times 10^{+9} (\text{Newton-m}^2) / (\text{amp}^2 \text{-sec}^2)$  is a constant that relates the dimensions of the parameters to each

other (refs. 17, 19) so that the quantity,  $a_e$ , is the propagation velocity of a small disturbance compression or expansion wave in meters/sec. If the charged particle being used is an ion, the various equations for mass and charge for a particle are obtained by changing the data for a single electron to the applicable multi-electron charge quantity and the mass of the electron from  $m_e$  to the appropriate mass-magnitude of the heavier particle. It is noted that the charged particles used in this paper are all electrons, because they have the largest charge-to-mass ratio of all particles, and as such, have the largest critical velocity, and the greatest possibility of being accelerated to velocities above the speed of light. If application is made to ions that have both a larger mass and a larger charge, the velocity of propagation of a small disturbance compression or expansion wave will be considerably reduced, and therefore will reduce the ability to accelerate heavier particles to velocities that are comparable with or that exceed the speed of light.

## **V. DESIGN OF ONE-DIMENSIONAL CHANNELS FOR TRANSITION FROM SUBCRITICAL TO SUPERCRITICAL FLOW VELOCITIES— STREAM OF NEUTRAL GAS**

### **A. Differential Equations**

The purpose of the study in this section is to define how one-dimensional steady-state channel flow fields of a neutral gas need to have their along-channel area distributions designed so that a transition in Mach number from subcritical to supersonic flow velocities will occur. That is, in the analysis to be presented, the flow of an electronically-neutral gas, like air, is studied to find out how the variations of cross-sectional size must be designed if a transition from sub- to supersonic stream velocities is to be achieved. It is assumed that the stream is steady with time and that it is at a temperature that is not near an extreme. It is also assumed that the stream velocity,  $U_a(x)$ , at a given station along the channel is largely in the  $x$  direction and approximately constant over each cross section of the channel. In this way, the flow field may be treated as a one-dimensional flow problem that does not vary with time. The pressure, density, and temperature of the gas are then related to one another by the equation of state as  $p_a = \rho_a R_g T_a$ , which, as stated previously, is based on the random thermal motions of air molecules. As the stream of air flows through such an idealized wind tunnel channel, the random thermal energy of the molecules is exchanged with the directed energy of the stream as it accelerates or decelerates. In this way, the bulk or total energy and momentum of the stream are continuously being transferred or exchanged between random molecular, or thermal energy, and the directed energy (velocity) of the stream. The objective of the analysis is to show that it is not just the pressure difference between the entrance and the exit of the channel that define the Mach number of the exit stream, but also that the cross-sectional area along the channel must also be defined in a certain way.

The analysis begins by simplification of the equations of motion from their expanded differential form written as the conservation of mass for a three-dimensional flow field for a compressible gas as

$$\partial\rho_a/\partial t + \partial\rho_a u_a/\partial x + \partial\rho_a v_a/\partial y + \partial\rho_a w_a/\partial z = 0 \quad (5a)$$

where the symbol,  $\rho_a$ , is again the density of a neutral gas like air, and  $u_a$ ,  $v_a$ , and  $w_a$  are respectively the velocity components of the stream of air in directions along the  $x$ ,  $y$ , and  $z$  coordinate axes. Because the flow fields being studied in this section are assumed to be steady with time, and to be approximately uniform over each cross-section of the wind tunnel channel, the conservation equations may be reduced to a function only of the stream direction,  $x$ , and magnitude. Such an assumption makes it possible to reduce the complexity of the analysis to a function of the one parameter,  $x$ , which is about the same as the stream direction. The rate of mass flow through the channel or stream tube may then be written as

$$\rho_a u_a A = \text{constant} \quad (5b)$$

where the parameter  $A$  is the cross-sectional area of the channel which is a function of  $x$ , the distance along the channel. Because the flow field has been reduced to a function only of the  $x$ -direction, which is aligned with the centerline of the wind tunnel channel, the equation for the conservation of mass may be written in differential form as

$$d\rho_a/\rho_a + du_a/u_a + dA/A = 0 \quad (5c)$$

In summary, it is assumed that any deviation of the local stream velocity from its average value,  $u_a$ , is small enough that products of perturbation values are negligible in comparison with the average value of the stream velocity,  $u_a$ . It is also assumed that viscous forces are negligible over the cross section of the stream, except for thin layers of gas along the walls of the channel where viscous effects become important. Because these regions are usually small when compared with the cross-sectional size of the channel, they are ignored as having a negligible effect on the average value of stream quantities. The  $x$ -component of the general momentum equation may then be written as

$$\rho_a[\partial u_a/\partial t + u_a \partial u_a/\partial x + v_a \partial u_a/\partial y] + \partial p_a/\partial x = 0 \quad (6a)$$

which, for steady stream velocities may be reduced to

$$\rho_a u_a du_a/dx + dp_a/dx = 0 \quad (6b)$$

for the one-dimensional flow field being considered.

Similarly, the conservation of energy, Eq. (7), which will not be used in the analysis to follow because no heat energy is added to or taken from the stream, is written in order to complete the set of equations often required to properly represent all of the properties of the stream. That is, the equation for the change of energy with time, the internal energy,  $E_a$ , and the work done on or by fluid plus any convection of heat may be written in equation form as,

$$dQ_a/dt = dE_a/dt + dE_k/dt + dW_a/dt + k_a \text{ Grad } T_a \quad (7)$$

where,

$Q_a$  = total energy

$T_a$  = temperature of air

$E_a$  = internal energy =  $C_v T_a$

$E_k$  = kinetic energy =  $\rho_a V^2/2$

$k_a$  = coefficient of conduction of heat

$\rho_a$  = density of air

$dW_a/dt$  = rate at which work is done by or on the fluid

In the analysis to follow, the equation for the energy of the stream of fluid is used only to specify that no heat is added or subtracted from the stream as it flows through the channel.

### **B. Effect of Variations in Size of Cross Section of Channel on Velocity and Mach Number -Stream of Neutral Gas**

It is first noted that, when the fluid is incompressible like a liquid, the velocity of the fluid in the channel is inversely proportional to the cross-sectional size of the channel,  $A$ , because the volume of the stream flowing through the channel is assumed to be a constant given by

$$\rho_a u_a A = \text{mass flow rate} = \text{constant} \quad (8a)$$

That is, when the gas in the channel,  $\rho_a$ , is incompressible and constant like a liquid, the stream velocity,  $u_a$ , changes inversely with the cross-sectional area,  $A$ , of the channel in order to keep the mass flow rate the same at all stations along the channel. If, however, the medium is a gas that is compressible, Eq. (8a) still applies, but the velocity, density, and pressure in the stream now all become variables in the stream as it changes velocity through the channel. The various parameters then depend not only on the local cross-sectional size of the channel, but are now also dependent on the previous history of the stream velocity and the cross-sectional size of the channel. As a consequence, the characteristics of the flow-field channel needed to bring about the transition of flow-field velocities from subcritical to supercritical must be designed so that their pressure flow fields move with the aerodynamic elements of the stream, and not by force fields that are fixed to a laboratory frame of reference, making acceleration of stream elements beyond supercritical stream velocities much more difficult.

The next step in the analysis begins with an expansion of the equation for the conservation of mass, Eq. (8a), to read (12)

$$d\rho_a/\rho_a + du_a/u_a + dA/A = 0 \quad (8b)$$

and the conservation of momentum as

$$u_a du_a + dp_a/\rho_a = 0 \quad (8c)$$

Similarly, the equation for the speed of sound at a given station in the fluid is written as

$$a_a^2 = dp_a/d\rho_a = \gamma p_a/\rho_a = \gamma R_g T_a \quad (8d)$$

Equation (8c) may then be rewritten by use of Eq. (8d) to become

$$u_a du_a + (dp_a/\rho_a)(a_a^2 dp_a/dp_a) = 0 \quad (8e)$$

or

$$u_a du_a + a_a^2 d\rho_a/\rho_a = 0 \quad (8f)$$

Now change the expression  $d\rho_a/\rho_a$  by use of Eq. (8b) to yield,

$$u_a du_a - a_a^2 (du_a/u_a + dA/A) = du_a(u_a - a_a^2/u_a) - dA/A = 0,$$

which may be rewritten as

$$(du_a/u_a)[(u_a^2/a_a^2) - 1] - dA/A = 0 \quad (8g)$$

or as

$$(du_a/u_a)[1 - M_a^2] = -dA/A \quad (8h)$$

where,  $M_a$  is the Mach number of the air in the channel at a given station. When  $M_a$  is less than one, the flow field is designated as subsonic, and the velocity of the stream,  $u_a$ , can only be increased by a decrease in the channel cross-sectional size with downstream distance. Such a result is the same as would occur with an incompressible fluid flowing through the channel. However, when Eq. (8h) is written as

$$(du_a/u_a)[M_a^2 - 1] = + dA/A \quad (8i)$$

the equation may be applied to supersonic (or supercritical) channel velocities. That is, if the Mach number,  $M_a$ , in the channel is greater than 1.0 (i.e., when the flow field is supersonic), Eq. (8i) indicates that the cross-sectional area of the channel must *increase* with downstream distance if the velocity of the stream is to *increase*! Such a result appears to be counterintuitive, but it is the correct interpretation as indicated by the number of successful supersonic wind tunnels that have been built on the guidelines indicated by Eqs. (8h) and (8i). The foregoing conclusions also assume that the pressure difference between the beginning of the channel and its exit station must be large enough to maintain the velocity distribution along the channel.

### C. Transition of Stream Velocities of Air from Less-Than to Greater-Than Critical

The foregoing analysis shows that a large pressure difference along the channel alone is not sufficient by itself to achieve a transition from subcritical to supercritical velocity. That is, the variation of the cross-sectional area of the channel along the duct must also follow a given sequence if supersonic (or supercritical) flow velocities are to be achieved. That is, if a transition from subsonic to supersonic velocities is to be brought about in the channel stream, the aerodynamic channel must have a properly designed shape, as shown in figures 2 and 4. The analysis indicates that the channel must first have a contracting cross-sectional area to accelerate the stream velocity up to a Mach number of one (i.e., usually referred to as a throat). The contracting channel must then be closely followed by an expanding cross-sectional area, that then further accelerates the flow field to velocities above a Mach number of one. For example, such a condition arises when the Mach number desired for the test section of the wind tunnel is near 1.0. If channel cross-sectional sizes are not properly sequenced, the Mach number and velocity of the flow field may be driven into an oscillation, from above to below a Mach number of one, rather than making a positive and smooth transition from subcritical to a supercritical velocity, without changing back and forth. A smooth transition is accomplished, however, if the smallest cross-sectional size occurs at the same streamwise location in the channel as where the

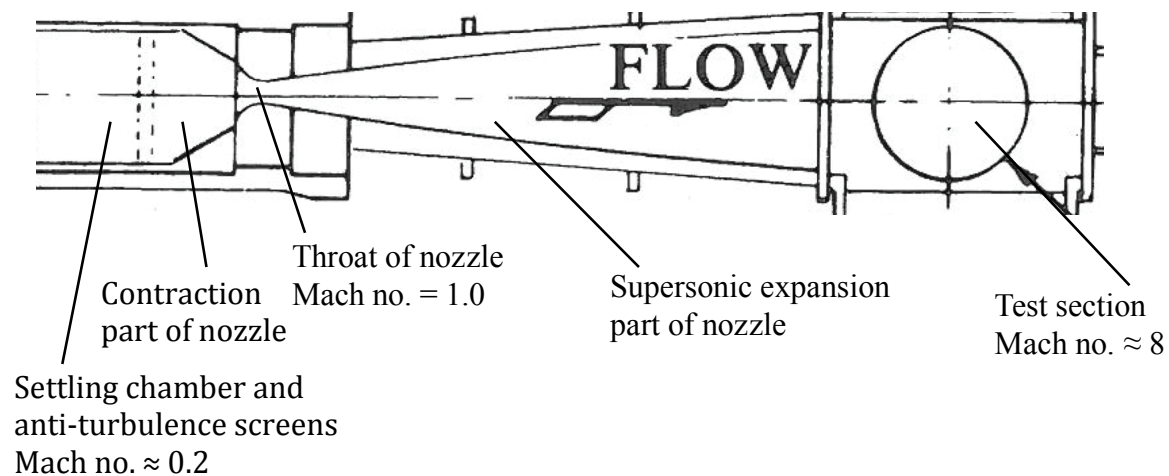


Figure 4. Diagram of a portion of wind tunnel circuit to illustrate how certain aspects of channel design must be made if the transition from subsonic to supersonic flow is to be accomplished. The transition is made at the smallest part of the throat of the nozzle where the stream Mach number goes through 1.0 on its way to a Mach number of 8.0. The expanding part of the channel downstream of the throat is designed to produce a uniform stream in the test section. This figure is a portion of the figure used to illustrate NASA Langley Research Center's Mach number 8 open-circuit non-return flow-through hypersonic wind tunnel (reproduced from page 269A of ref. 2). A more complete picture of the facility is shown in figure 2.

Mach number is equal to one; i.e.,  $M_a = 1.0$ . That is, at the minimum or throat station in the channel, the velocity of the stream must aggressively change from being first slightly below and then slightly above its critical velocity (i.e.,  $M_a = 1.0$ ), so that the transition from subsonic to supersonic flow velocities will occur smoothly without flow-field oscillations (e.g., figure 4).

It is recommended that one of the beginning experiments consist of the development of a wind-tunnel-shaped channel like the one shown in figure 4 that has been developed and prepared for the flow of a stream of electrons.

#### **D. Overview of Channel Dynamics**

If it is desired that the near sonic stream velocity at the throat of the channel be maintained throughout the test section, then that part of the channel must be built with porous walls. That is, the correct way to build test facilities for aerodynamic studies at and through the critical and near-critical transonic Mach number range (i.e.,  $M_a \approx 1$ ) was formulated by John Stack of NACA Langley Research Laboratory in the early 1950s. His solution was to use porous walls for the test section part of the channel so that when aerodynamic disturbances from a test model cause pressure waves from a non-uniformity in the airstream to encounter a wall of the channel, a portion of the disturbance would pass out of the channel by flowing through the porous openings in the channel wall into a plenum chamber that surrounds the test section part of the circuit. Because the plenum chamber is kept at a slightly lower pressure than the test region part of the channel, the boundary layers on each wall of the test section are drawn off along with any unwanted disturbance waves. In this way, the flow fields of transonic wind tunnels become steady with time and take on the character of a uniform flow field that enables the simulation of an aircraft flying through the atmosphere at any test Mach number in the facility, whether it is at or near one.

In general, however, the flow-field problems addressed here are devoted to stream velocities well above the critical velocity for the stream so that transonic problems will be avoided. A smooth transition from subsonic to supersonic Mach numbers in a channel is then facilitated by the smooth and well-designed distributions of cross-sectional area shown for the channel in figure 4. It is noted that the channel size varies smoothly from a minimum or throat area and then into a diverging section to accommodate or to bring about the expansion of the stream cross section for the desired supersonic flow field. Of course, the tunnel drive system must be able to maintain the required pressure differences along the channel length at large enough values to accommodate those needed for the Mach number range that matches the area distribution along the channel. That is, the various parts of the entire wind tunnel facility, like the turning vanes, anti-turbulence screens, and pumps or turbines need to be designed so that they provide the pressure differences and flow rates needed to produce the velocity and stream quality needed by the area ratios of the test section part of the channel. These “other parts” of the facility may be of a wide variety of designs and are usually based on the overall needs of the wind tunnel channel and its test section (e.g., pp. 50–84 of ref. 1).

### E. Linearized Partial Differential Equations for Compressible Flow of Neutral Gas

Before large capacity electronic computers became available for solution of flow-field problems, approximate solutions to the complete differential equations were obtained by use of linearized steady-state partial differential equations that resemble Laplace's equation. They can be written for subsonic flow fields (refs. 3–11) as

$$(1 - M_a^2)\phi_{xx} + \phi_{yy} + \phi_{zz} = 0 \quad (9a)$$

and for supersonic flow fields as

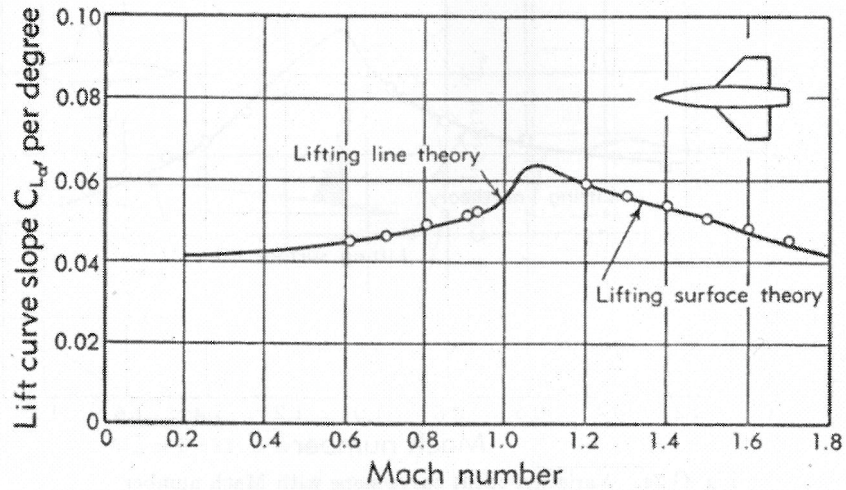
$$(M_a^2 - 1)\phi_{xx} - \phi_{yy} - \phi_{zz} = 0 \quad (9b)$$

where  $M_a = U_a/a_a$  is the free stream Mach number for air. The various derivatives of  $\phi$  represent the derivatives of the velocity component in directions along the three coordinate directions, which are assumed to all be a small fraction of the magnitude of the free-stream velocity,  $U_a$ . When large capacity and high-speed computers became available, numerical methods were developed that can now solve for almost any aerodynamic problem associated with the flow field around an aerodynamic shape, whether or not the aircraft is inside a wind tunnel.

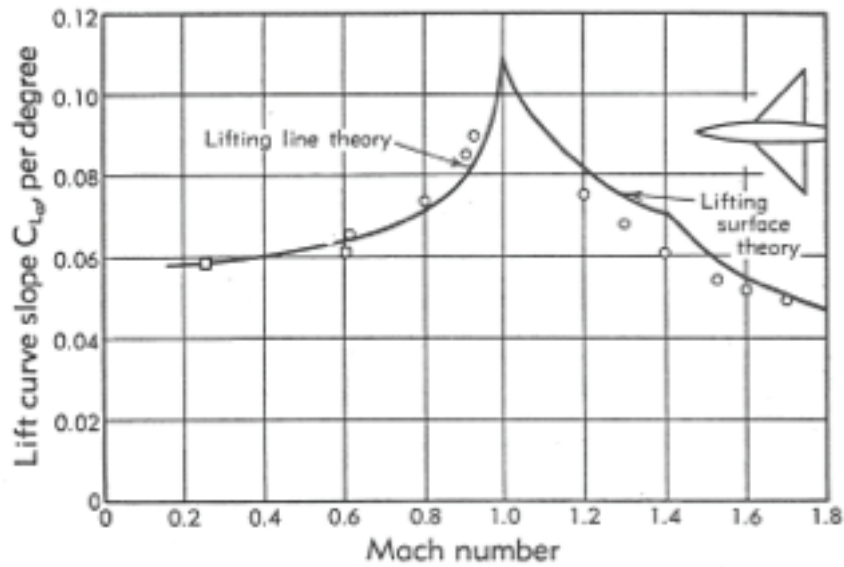
### F. Examples of Wind Tunnel Data At and Near Critical Velocity

As pointed out in preceding sections, supersonic wind tunnels require that their channel have a contracting cross-sectional area followed by an expanding cross-sectional area just beyond a throat region, to establish a continuously accelerating flow field. As also mentioned in the previous section, if the Mach number desired for the test section of the wind tunnel is near 1.0, the Mach number and velocity of the flow field will oscillate uncontrollably, rather than make a smooth transition to the desired flow velocity, if certain design features are not used. A smooth transition is accomplished, however, if a concept formulated and put into practice by John Stack (while Stack was at the NACA Langley Research Laboratory in the early 1950s). As mentioned previously, his solution was to use porous walls (instead of solid walls) for the test section part of wind tunnels when the Mach number was near one. An example of aerodynamic data, in very good agreement with results obtained for two idealized wing-body combinations (ref. 9), obtained in a properly designed transonic wind tunnel is shown in figure 5a and 5b; the circular symbols represent experimental data points.

Prior to the invention of smoothly flowing transonic wind tunnels by Stack, the taking of measurements like the ones shown in figure 5, and the development of theoretical models for the transonic flow fields were not possible.



a. Clipped wing-tip aspect ratio = 2.



b. Wing aspect ratio = 4.

Figure 5. Comparison of predicted and measured lift-curve slope as taken in a transonic wind tunnel as a function of stream Mach number for two wing-body combinations when one wing is a clipped triangular wing-tip configuration with an aspect ratio of four, and the other is not, as indicated on the figure in plan view. (From figures G,2e and G,2f on pages 802–3 in ref. 9.)

### G. Return-Flow Part of Wind Tunnel Circuits

At some station or stations around the circuit of subsonic and supersonic wind tunnels, power must be added to the airstream in order to provide the needed pressure differences across the sub- and supersonic acceleration parts of the flow-field circuits. The power levels needed are generally more than just adequate to overcome any inertia or dissipation forces that occur. The amount of power that needs to be added depends on the nature of the model being studied and on

the nature of the circuit. Of course, the power required increases with the complexity of the tunnel circuit, and with the velocity of the airstream, to roughly the third power of the stream velocity in the test section. If the facility is to be operated on a continuous basis, further power must generally be added to the circuit to overcome the energy needed to push the air through an air exchanger or cooler that either removes the unwanted heat or exchanges the air with the atmosphere itself to maintain satisfactory operating conditions in the test section of the facility.

## VI. DESIGN OF ONE-DIMENSIONAL CHANNELS FOR TRANSITION FROM SUBCRITICAL TO SUPERCRITICAL FLOW VELOCITIES— STREAM OF ELECTRON GAS

It is first noted that the analysis to follow is almost the same as the one that was developed in the previous section for wind tunnel (aerodynamic) channels. This very similar analysis is presented in the same format to emphasize the similarity of the two flow fields and to display the small differences that also exist whenever the structure of the equation of state (or of the speed of sound) is involved.

### A. Differential Equations

A relationship for the equation of state for the idealized stream of an electron gas stream being explored here is derived in the Appendix of this paper as

$$p_e = \rho_e^{2/3} [e^2 / (4\pi K_0 m_e^{1/3})^2] = 20820.0 \rho_e^{2/3} \quad (10a)$$

or

$$p_e / \rho_e^{2/3} = \text{Constant} = 20820.0 \quad (10b)$$

It is noted that temperature is not a factor in Eqs. (10a) or (10b) because it is assumed that the electrons in the gas are 'cold' so that each electron has no motion of its own, and only moves as a part of the bulk motion in the fluid, as assumed in the Appendix herein, where the structure of the gas is specified. The velocity of a small disturbance wave through an electron gas is then given by the expression discussed previously as

$$a_e = (dp_e / d\rho_e)^{1/2} = (e/d_e) / (4\pi K_0 m_e)^{1/2} = E_K / d_e$$

where  $E_K^2 = e^2 / (4\pi K_0 m_e)$  or,  $E_K = 1.592$ , so that

$$a_e = 1.592 / d_e \text{ m/sec} \quad (10c)$$

where the parameter,  $d_e$ , is the undisturbed distance between electron centers that make up the electron gas. It is again noted that the electron gas being used in the present study has zero thermal motions and sustains its character as a gas because of the presence of forces of repulsion between the electrons themselves. The channel through which the electrons flow is assumed to

be composed of an insulating material, like glass, that is strong enough to contain the gas and any other loads associated with the stream. Electromagnetic fields might also be used to control stream boundaries: e.g. ref.19.

The same type of analysis that was carried on streams of air in a one-dimensional channel is now carried out for a stream of an electron gas. An expanded form of the differential equation for the conservation of mass for the three-dimensional flow of a compressible electron gas is written here as

$$\partial \rho_e / \partial t + \partial \rho_e u_e / \partial x + \partial \rho_e v_e / \partial y + \partial \rho_e w_e / \partial z = 0 \quad (10d)$$

where, as before, the symbol  $\rho_e$ , is the density of the electron gas and  $u_e$ ,  $v_e$  and  $w_e$  are respectively the velocity components of the electron gas along the x, y, and z coordinate axes. Again, because the flow fields being studied in this section of the paper are assumed to be steady with time and to be approximately uniform over each cross section of the flow-field channel, the conservation of mass for the flow field in the channel may again be written as,

$$\rho_e u_e A = \text{constant} \quad (10e)$$

Because the flow field has been reduced to a function only of the x-direction, which is aligned with the centerline of the flow-field channel, the equation for the conservation of mass may also be written in differential form as

$$d\rho_e / \rho_e + du_e / u_e + dA / A = 0 \quad (10f)$$

The differential equation written for the conservation of momentum again assumes that any deviations of the stream velocity from its average value,  $u_e$ , at each station along the channel is so small that perturbation values are negligible in comparison with the local average value. It is also again assumed that viscous forces are negligible over the cross section of the stream except for thin layers of gas along the walls of the channel, so that the x-component of the general momentum equation may be written as

$$\rho_e [\partial u_e / \partial t + u_e \partial u_e / \partial x + v_e \partial u_e / \partial y] + \partial p_e / \partial x = 0 \quad (10g)$$

and, for one-dimensional flow fields, may be reduced to

$$\rho_e u_e du_e / dx + dp_e / dx = 0 \quad (10h)$$

## **B. Effect of Variations in Size of Cross Section of Channel on Velocity and Mach Number**

As with the flow fields along the channels of wind tunnel airstreams, the variations in the velocity of the medium (or stream of electrons in the present case) depends on the cross-sectional area along the channel. The discussion to follow is about the same as presented previously for

wind tunnel channels, and will treat the influence of variations in the cross-sectional size of the channel on the electron Mach number,  $M_e$ , of the gas stream in the channel, as given by

$$M_e = u_e/a_e \quad (10i)$$

where ‘ $u_e$ ’ is the velocity of the charged particles in the stream, and ‘ $a_e$ ’ is the speed of propagation of a small disturbance wave through the electron gas in the channel as given by

$$dp_e/d\rho_e = a_e^2 \quad (10j)$$

where the equation of state, or relationship between the pressure and density for an electron gas is given by

$$p_e/\rho_e^{2/3} = \text{Constant} = 20820.0 \quad (10k)$$

As with the channel in the wind tunnel flow field discussed previously, the conservation of mass at low velocities moves as an incompressible fluid, or liquid, so that the velocity of the fluid in the channel is inversely proportional to the cross-sectional size of the channel because the volume of the stream flowing through the channel is assumed to be at a constant rate given by

$$\rho_e u_e A = \text{flow rate} = \text{constant} \quad (10l)$$

When the density,  $\rho_e$ , of the gas in the channel is incompressible and constant, like a liquid, the flow rate,  $u_e$ , changes inversely with the cross-sectional area of the channel. If however, the fluid is a gas, which is compressible, the relationship between the pressure and the density then becomes more complex, and an equation of state for an electron gas is needed; e.g., Eq. (10a). As with the airstream in a wind tunnel, the various flow-field parameters again then depend not only the cross-sectional size of the channel but also on the previous history of the cross-sectional size of the channel.

The analysis begins with Eq. (10a) being rewritten as

$$dp_e/\rho_e + du_e/u_e + dA/A = 0 \quad (10m)$$

The speed of a small disturbance wave through an electron gas is given by

$$dp_e/d\rho_e = a_e^2 = E_K^2/d_e^2 \quad (10n)$$

and the equation for the conservation of momentum is given by

$$\rho_e u_e du_e/dx + dp_e/dx = 0 \quad (10o)$$

The foregoing equations then allow an equation like the one developed for the flow of air in wind tunnel channels to also be written for streams of charged particles as

$$(du_e/u_e)[1 - M_e^2] = -dA/A \quad (10p)$$

where,  $M_e$  is the Mach number of the electron gas in the channel at a given station. The differential equation presented by Eq. (10m) indicates that, just like the aerodynamic case, when  $M_e$  is less than one the stream velocity can only be increased further by an decrease in the cross-sectional area of the channel. As with a channel flowing with air, when the Mach number,  $M_e$ , is greater than one, the differential equation may be re-written as

$$(du_e/u_e)[M_e^2 - 1] = +dA/A \quad (10q)$$

so that it indicates that the velocity  $u_e$  can then only be increased by an increase in the cross-sectional area of the channel. Of, course, when  $M_e = 1$  and it is desired to increase or decrease the stream velocity, Eq. (9k) provides no guidance. In the case of wind tunnel airstreams it was found that converging and diverging sections connected by a “throat” region, as with neutral gases, provides the needed design. That is, the technique used for wind tunnel design also applies to the acceleration of charged particles from subcritical to supercritical velocities.

### C. Return-Flow Part of Wind Tunnel Circuits

When the stream being used in the aerodynamic facility is not a neutral gas, but one composed of electrons, the facility must also be equipped with devices that properly control and deal with the presence of accumulated and moving electrical charge distributions that the electron stream may possess. As mentioned previously, the channel through which the electrons flow is assumed to be composed of an insulating material, like glass, that is strong enough to contain the gas and the electromagnetic loads of the stream. Because the flow-field stream being designed is composed of only electrons it is necessary to accelerate the stream of electrons through its high-speed structure from initial acceleration to a target location without disruption. For this purpose, some sort of device (or circuit) must parallel the planned channel flow field to serve as a return route for the electrical charge that travels with the stream in the channel. The return route or circuit will need to be designed with the equipment to transport the electrical charges back to the initial point of release. The same charges, or electric current, is thereby escorted back to the beginning of its trip through the channel where it is regenerated for another trip along the planned circuit as a stream of charged particles (i.e., a stream of electrons). One of the early methods used in the operation of electron tubes (ref. 18) was the use of special screens as electron gathering tools, like those used in vacuum electron tubes in the distant past.

## VII. MACH WAVES—A TOOL FOR THE ANALYSIS OF SUPERCRITICAL AERODYNAMIC FLOW FIELDS

The foregoing discussions have been devoted mostly to one-dimensional flow fields in order to provide simple illustrations of fundamental aerodynamic processes, and of channel designs that do and do not make the transition from subcritical (i.e.,  $M_a < 1$  and  $M_e < 1$ ) to supercritical (i.e.,  $M_a > 1$  and  $M_e > 1$ ) stream velocities. Now that the effect of channel cross-sectional size variations on stream velocity has been clarified, it remains to provide a theoretical tool that efficiently makes the basic one-dimensional stream concept into a usable two- or three-dimensional tool for the analysis of more complex stream configurations. The process to be followed is to first design a tool that is helpful in the theoretical treatment of two- and three-dimensional aerodynamic flow fields. The one chosen has been associated with the design and function of wind tunnel facilities and of aircraft for some time. After a derivation has been presented on the properties and attributes of Mach waves, solutions to several supersonic flow fields are presented to indicate the potential benefits that become available when the solutions developed for aerodynamic flow fields become available, and that can also be extended/adapted to comparable flow fields composed of electrons. It is noted that the transition of the flow-field velocities from subcritical to supercritical must be designed so that their pressure flow fields move with the aerodynamic elements of the stream. In contrast, streams of charged particles are presently usually driven by use of force fields that are fixed to a laboratory frame of reference, making acceleration of stream elements beyond supercritical stream velocities much more difficult.

### A. Aerodynamic Problem in Need of Solution

In the early 1900s, it was realized in Europe that theoretical tools were needed to assist in the development of wind tunnels and of aircraft that would function at supersonic, as well as subsonic, velocities. Useable solutions were found by simplification of target flow fields that had complex interacting processes, into ones that were simple enough to solve theoretically (refs. 11–27). For example, figure 6 illustrates the two-dimensional supersonic flow of a stream of air around a smoothly contoured turn that might occur on the wall of a wind tunnel or on the surface of an aircraft. The development of such a theoretical flow field begins with a set of nearly horizontal streamlines that form lines and curve downward to follow a wall as if turning a corner. The upward running and slanting lines labeled  $C_+$  in figure 6 represent Mach waves wherein each has its origin on the lower boundary or floor of the air stream, and then slopes downstream. Although the flow field appears simple, it is actually a two-dimensional steady-state flow problem that is too difficult to solve without the help of a Mach wave tool, whose development is described next.

The Mach wave concept began its development by first changing the rounded corner shown in figure 6 into several small, sharp turns to produce a sequence of corners that accomplish the same turning angle as produced by the much larger rounded corner. Because the flow field is supersonic (or supercritical) everywhere, each “corner flow field” may be treated as a separate

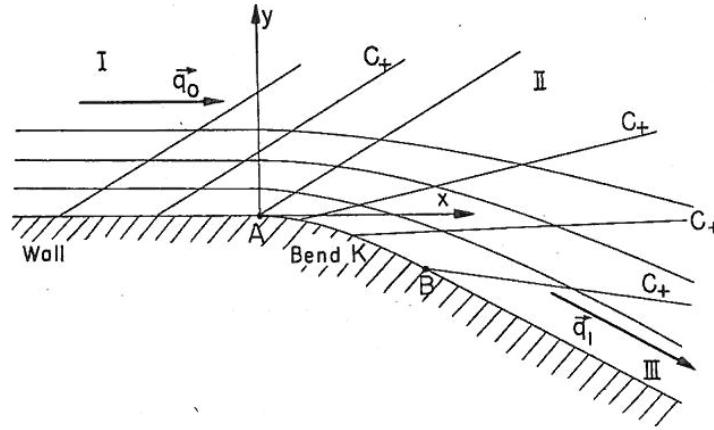


Figure 6. Diagram of a supersonic flow field around a single, smooth aerodynamic turn like the ones that often occur along wind tunnel walls or on the surfaces of aircraft (from fig. 14 of Courant and Friedrichs ref. 13).

and as an isolated sharp corner. Because the airstream is assumed to be everywhere supersonic, these simplifications lead to a flow-field model where each corner flow field may then be treated as a one-dimensional flow field. That is, because the flow-field parameters are constant along each ray (a Mach wave) that has its lower end attached to the corner. It is also noted that the flow field is entirely supersonic without any crossing or intersecting Mach waves. As a result, the flow field around each small corner is a flow field by itself, because each is isolated from the others, and may be treated separately.

The smoothly contoured surface shown in figure 6 may then be considered as a large number of very small step-wise corners where each may be solved by treating the sequence of corners as a sequence of isolated small-amplitude corners. Each corner then consists of one supersonic corner flow field that allows or promotes a small turn in the airstream that promotes the airstream to pass onto the next small corner, so that each corner flow field again performs as an isolated corner flow field, etc. That is, the solution for one corner flow field passes a stream structure on to the next corner where it becomes the initial condition for another following corner flow field.

In each of the foregoing corner flow fields, only a lower (as shown), or an upper boundary, but not both, is permitted to exist in order to be certain that only one set of Mach waves, and no reflected waves, are present in each corner flow field. Only the lower boundary case will be considered because it is essentially an upside-down version of an upper-boundary solution. It must be remembered, however, that if a second surface is present in the flow field, its presence produces a second set of Mach waves that will probably interact with the other corner flow field to produce a complex two-dimensional flow field. Such a flow field requires a more complex set of tools that are available in the literature, and that will not be discussed at this time. A subsection to follow explains how those kinds of flow fields can be solved by use of a method that contains interacting Mach wave flow fields. This more complex numerical method involves the interaction of Mach waves on a mesh that develops as the solution marches across the flow field. This technique is known as the method of characteristics (refs. 11–26).

## B. Mach Waves—A Theoretical Relationship Between Stream Velocity, $V_1$ , and Small Flow-Turning Angle, $d\theta$ , When Gas Is Air

The differential form of the flow field across a Mach wave (or a small fan-shaped group or bundle of Mach waves) as illustrated in figure 7, is now used to develop the theoretical concept of Mach waves. A stream of air is assumed to be flowing from left to right at a supersonic velocity,  $V_1$ , in a channel whose lower surface makes a small, sharp, downward turn,  $d\theta$ . The infinitesimal corner model shown in figure 7 is now used to help guide the development of a differential expression for small angular turns that can then be integrated and/or relocated for the larger turns that are more practical for actual flow fields. The flow-field increment in stream velocity,  $dV_n$ , and the corresponding stream angle change,  $d\theta$ , associated with this infinitesimal turn has become known as a Mach wave relationship.

The small-angle turn,  $d\theta$ , is the aerodynamic disturbance that initiates and supports the aerodynamic Mach wave process that propagates diagonally across the supersonic stream by means of a pressure or Mach wave that slopes across the flow field at the angle,  $\beta_1$ , defined as,

$$\sin \beta_1 = a/U_\infty = 1/M_{a1} \quad (11a)$$

where ‘a’ is the speed of sound of the air in the stream (the subscript ‘a’ for air is not applied here to simplify the nomenclature), and  $U_\infty$  is the velocity of the stream upstream of the Mach wave, and  $M_{a1}$  is the Mach number of the stream just before the flow field begins its turn. The parameter,  $M_{a1}$ , and the angle,  $\beta_1$ , are known as the Mach number, and Mach angle, after Ernst Mach, the first person to describe the tool and to explain its function in supersonic flow fields (refs. 16, 21–26). In order to reduce the clutter in the equations and in the figures to follow, the subscript “a” will often not be used in the derivation to indicate that the test gas is air.

The structure and function of Mach waves are now reproduced here to illustrate the development of a useful tool that enables the development of flow-field solutions for a wide variety of aerodynamic surfaces, and to set up the same type of analysis for streams of electrons. It is first noted that the two-dimensional flow field shown in figure 7 has been reduced to a one-dimensional one that depends only on the angle of the ray to the horizontal,  $\phi = \theta + \beta$ , and not on the linear distance from the corner in any direction. In figure 7, the parameter  $d\theta$  represents a small increment in the angle of the stream direction at the corner relative to the horizontal approach direction, and  $\beta_1 = \sin^{-1} (a_1/U_1)$  is the Mach angle relative to the stream direction upstream of the corner. It is also observed that, no matter the magnitude of the turn, the flow field remains one-dimensional in character as long as the magnitude of the stream velocity is supersonic (and not subsonic), and the flow-field parameters are constant along the rays through the corner. In this way, and as mentioned previously, the two-dimensional nature of the flow field as a supersonic stream over a rounded corner is changed into a series of small/infinitesimal sharp turns that are each approximated by a one-dimensional small sharp corner, so that each may be treated as a one-dimensional problem.

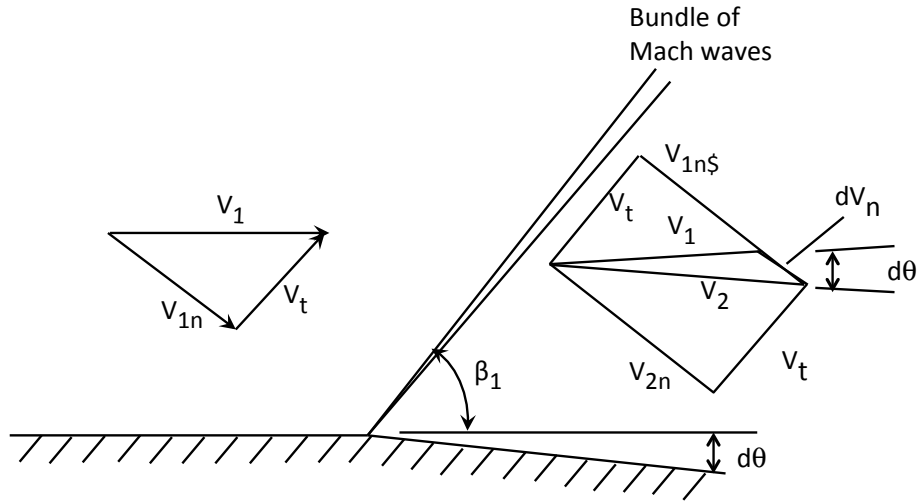


Figure 7. Diagram of velocity components relative to entry and exit of a stream of air from a Mach wave (or small bundle of Mach waves) to show how the small-amplitude components perpendicular to the Mach wave simultaneously produce a change in the velocity, or an acceleration,  $dV_n$ , of the stream component perpendicular to the Mach wave bundle, and thereby an angular turn,  $d\theta$ , in the flow direction of the stream (refs. 11–14 and 21–26).

As indicated in figure 7, because the velocity of the stream is supercritical, or supersonic, the presence of the downward turn in the floor of the channel is not propagated immediately throughout the entire stream, but only at and along the diagonal aerodynamic surface provided by the Mach wave (or the small bundle of Mach waves that it represents). The action of the Mach wave bundle is contained between the two Mach waves, defined as the one on its upstream side by the upstream Mach number,  $M_1$ , and one on the downstream side by the downstream Mach number,  $M_2$ . A wedge-shaped bundle of infinitesimal Mach waves is assumed to be contained between the upstream Mach wave and the downstream Mach wave, both anchored at the corner, in order to promote the turn at and around the corner.

The downstream Mach wave boundary is tilted more to the right than the upstream Mach wave for two reasons. The first reason is because the stream angle is tilted downward by the stream angle at  $d\theta$ , and the second reason is because the Mach angle of the stream downstream of the corner is larger than that of the upstream flow field, so that its Mach angle is smaller, because of its larger stream velocity there. Even though the Mach wave has an increased depth for the foregoing reasons, the Mach wave bundle or fan is usually treated as a single aerodynamic surface, instead of a fan-shaped region. It is along this aerodynamic ‘surface’ that the presence of the corner is eventually communicated along the diagonal Mach wave path to each part of the stream above the corner.

In brief, the Mach wave is assumed to serve as the aerodynamic tool/mechanism that simultaneously turns and accelerates the airstream from its horizontal velocity,  $V_1$ , in front of the Mach wave, to an increased velocity,  $V_2$ , just downstream of the Mach wave, as it is driven by the change in direction,  $d\theta$ , of the stream. That is, the stream is accelerated and turned by its

passage through the small fan of Mach waves so that the stream follows the downward slope of the wall that exists downstream of the corner.

The size of the angular turn of the Mach wave (or wave bundle), as indicated in figure 7, is given on its upstream side by  $\beta_1 = \sin^{-1}(a_1 / V_1)$ , where the subscript “1” indicates a station just upstream of the Mach wave or wave bundle. Similarly, the Mach wave just downstream of the Mach wave bundle is labeled as  $\beta_2 = \sin^{-1}(a_2 / V_2)$ , as indicated in the figure. These two Mach waves contain the aerodynamic turn and acceleration mechanism,  $dV_n$ , of the stream that communicates to the oncoming stream that a corner is present in the flow field and that the airstream must turn downward by the angle,  $d\theta$ , in order to follow the lower boundary of the airstream.

As illustrated in figure 7, expressions for the aerodynamic features of the Mach wave indicate that the component of the stream velocity parallel to the Mach wave is unchanged as the air crosses the wave, because aerodynamic forces cannot influence fluid particles travelling in a direction parallel to, or along, the surface of the Mach wave. However, the magnitude of the velocity component of the oncoming stream that is perpendicular to the face of the Mach wave is changed by the vector addition,  $dV_n$ . That component of the stream velocity is perpendicular to the Mach wave surface as indicated in figure 7. In order to develop a theoretical relationship for the aerodynamics of the Mach wave, the change in velocity is shown as a short vector,  $dV_n$ , between the tips of vectors  $V_1$  and  $V_2$ . The subscript “n” denotes that the vector change in the stream velocity is only in the direction normal or perpendicular to the front of the Mach wave. In the theory, and as a perfect gas, each streamline becomes aligned with the direction of the channel floor downstream of the corner, after it has passed through the wave.

The intent of the sketch shown in figure 7 is to first develop an incremental solution/model for the problem of a single, small bundle of Mach waves into a differential equation that can be integrated for entire flow fields that are more realistic, and more complex. In the foregoing analysis, it is again assumed that the downstream pressure in the vicinity of the corner, and the viscosity of the fluid are small enough that the streamlines around small or large turns with rounded or sharp corners do not separate from the boundary walls, but follow the surface as an uninterrupted streamline. The turn is then executed as a combined change in direction, or turning angle,  $d\theta$ , as it expands and accelerates around a small corner as indicated in figure 7. It is also assumed that the turn and expansion are executed as an isentropic event without loss of energy that is sometimes brought about by dissipation processes that occur when viscosity or strong compression waves are present. As a reminder, if the stream velocity had been subcritical (or subsonic), no compression or expansion waves would have been generated.

### **C. Analysis of Mach Wave for Small Angular Changes in Stream Angle**

Because it is the nature of Mach waves that they can only impart velocity changes in a direction that is perpendicular to the front face of the wave, the action of the Mach wave can be applied to the stream of air as a change only when the component of the velocity is perpendicular to the wave front. It does not influence the velocity component parallel to the wave front, which is

unchanged as the gas flows through any of the Mach waves in an expansion fan. In equation form, the conservation of mass across the wave may then be written as

$$\rho V_{1n} = (\rho + d\rho)(V_{1n} + dV_{1n}) \quad (11b)$$

In Eq. (11b) the subscript '1' denotes the station that is just upstream of the wave, and the subscript 'n' denotes that the vector is normal or perpendicular to the Mach wave. The letter 'd' is used to indicate a differential or incremental change in the parameter as it proceeds from one side of the wave to the other. In other words, the letter 'd' is used to indicate the fact that they are small increments or differentials. When products of differentials are ignored, Eq. (11b) becomes

$$V_{1n} d\rho + \rho dV_{1n} = 0 \quad (11c)$$

Similarly, conservation of momentum across and parallel to the wave requires that

$$\rho V_{1n} V_{1t} = (\rho + d\rho)(V_{1n} + dV_{1n}) V_{2t} \quad (11d)$$

and, due to the fact that Mach waves do not impart a change to the velocity components parallel to the Mach wave, they remain the same across the wave as

$$V_{1t} = V_{2t} \quad (11e)$$

which specifies that the component of velocity tangential or parallel to the wave does not change when the air moves across the wave from the upstream to the downstream side of a Mach wave. Similarly, the conservation of momentum perpendicular to the wave requires that

$$V_{1n} dV_{1n} + dp/\rho = 0 \quad (11f)$$

Now combine Eq. (11d) and Eq. (11e) to yield,

$$V_{1n}^2 = dp/d\rho = \alpha_1^2 \quad (11g)$$

Equation (11g) confirms the fact that the component of the velocity perpendicular to the Mach wave is sonic on the upstream side of the Mach wave.

Because the component of the velocity parallel to the Mach wave is the same on both sides of the wave, the component of the stream velocity parallel to the wave may be written as  $V_{1t} = V_{2t}$ . The magnitude of the upstream velocity component in a direction perpendicular to the Mach wave is given by  $V_{1n} = V_1 \sin \beta_1$  or, because the velocity  $V_{1n}$  must be equal to the speed of sound on the upstream side of the Mach wave,

$$\sin \beta_1 = a_1 / V_1 = 1/M_1 \quad (11h)$$

If the total velocity,  $V_2$ , of the airstream downstream of the Mach wave is to be parallel to the slope,  $d\theta$ , of the floor downstream of the corner, the velocity increment normal to the Mach wave must be increased by the amount given by  $V_1 d\theta$ . As indicated in figure 7, the product of the incremental change in the direction of the stream,  $d\theta$ , of the velocity vector,  $V_2$ , downstream of the Mach wave is equal to the product

$$V_2 d\theta = dV_1 \cos \beta_1 \approx dV_2 \cos \beta_1 \quad (11i)$$

When the angular change,  $d\theta$ , and the velocity change,  $dV$ , are taken to infinitesimal amounts,

$$dV = dV_n V_1 \quad (11j)$$

A relationship between  $dV$  and  $d\theta$  has been produced and maybe written as

$$dV/V = \sin \beta_1 d\theta / \cos \beta_1 = \tan \beta_1 d\theta = d\theta (M_1^2 - 1)^{1/2} \quad (11k)$$

or

$$d\theta = dV / [V(M_1^2 - 1)^{1/2}] \quad (11l)$$

so that the angular change in the flow direction,  $d\theta$ , is now a function of the velocity,  $V$ , and its increase,  $dV$ .

#### **D. Use of Reservoir Conditions to Relate Flow-Field Parameters to Each Other for Integration of Mach Wave Relationship for Air**

A relationship between the Mach number in air,  $M_1$ , and the speed of sound or temperature, is needed if the relationship (11l) is to be integrated for flow fields that make finite, and sometimes large-angle turns about sharp corners. Such a relationship has been derived by use of the reservoir temperature as a unifying parameter for the velocity and Mach number in order to build a unifying parameter for Eq. (11l) so that it can be integrated. Such a unifying parameter is developed from the ambient and total temperatures of the airstream by means of the energy equation (ref. 12), written as

$$T_o/T_a = 1 + M_a^2(\gamma_a - 1)/2 = \gamma R T_{ao} / \gamma R T_a = a_{ao}^2 / a_a^2 \quad (11m)$$

where  $\gamma_a$  is the ratio of specific heats for air as  $C_p/C_v$ . The subscript "a" for air is now added to the appropriate parameters because, as will be seen in a following section, the analysis presented for air and for an electron gas now become different from each other. Because the stagnation temperature of the stream,  $T_o$ , is conserved throughout the event, Eq. (11m) ties together the local velocity and the speed of sound. Therefore, the Mach numbers, which are all dependent on each other through the local temperature, are a quantity that does not yet exist for streams of electrons. Integration of Eq. (11k) or Eq. (11l) is, therefore, facilitated by conversion of all of the parameters to a common variable, like temperature. The presentation in reference 12 makes such an adjustment and was thereby able to then integrate Eq. (11l) for an analytical solution based on

tabulated trigonometric functions. By development of a relationship between the velocity parameter,  $V$ , and its thermodynamic parameters, Eq. (11l) can be integrated so that the flow turning angle,  $\theta$ , becomes a function of stream velocity or Mach number. Equation (11m) is the relationship that fulfills the need by use of the observation that the stagnation temperature of the isentropic flow field,  $T_0$ , and its corresponding speed of sound,  $a^* = 0.913a_0$ , where,  $a_0 = (\gamma RT_0)^{1/2}$ . In contrast, the Mach number  $M$  and the speed of sound,  $a$ , both change with the temperature and velocity of the local stream. Therefore, the  $a^*$  parameter provides a ‘durable’ relationship that can be used for the next step in the analysis is the relationship as,

$$(V/a^*)^2 = M_a^{*2} \quad (11n)$$

where the relationship between the two forms of the Mach number is given by

$$M_a^{*2} = (\gamma+1)/(\gamma-1 + 2/M_a^2) \quad (11o)$$

or

$$M_a^2 = 2 M_a^{*2} / [\gamma+1 - (\gamma-1) M_a^{*2}] \quad (11p)$$

$$d\theta_a = \{ [M_a^{*2} - 1] / [1 - ((\gamma-1)/(\gamma+1)) M_a^{*2}] \} \{ dM_a^* / M_a^* \} \quad (11q)$$

This relationship makes it possible to convert Eq. (11i) into a form that relates the angular change,  $d\theta$ , to a change in  $M^*$ , so that Eq. (11j) can be integrated; see reference 12 for the details of the analysis and tabulated values that relate downstream Mach number to turning angle,  $\theta_a$ .

### **E. Application of Differential Increment of Mach Waves to Prandtl-Meyer Expansion Fans**

Integration of Eq. (11l) begins at the station where the stream angle,  $\theta_a$ , is zero, and where the Mach number,  $M_a$  is one, and where the flow angle,  $\theta_a$ , is zero. A relationship between Mach number,  $M_a$ , and the flow deflection angle,  $\theta_a$ , as derived in terms of trigonometric functions, is presented on page 215 of reference 12. Tabulated results for the deflection angle of airstreams,  $\theta_a$ , and the Mach number,  $M_a$ , are also presented by Sauer (page 90 of ref. 11). Graphical results are also presented on a loose-leaf page in a pocket of reference 12 (Liepmann and Puckett) and on page 460 of reference 14 (Shapiro).

As a consequence, the Mach waves that make up the “expansion fan” of Mach lines and that serve as the expansion fan in Prandtl-Meyer flow fields bring about a continuous series of incremental velocity changes all at the same corner to form an expansion fan like the one shown in figure 8. The flow field presented produces a fan-shaped set of waves throughout the volume of the fan with all of the active Mach waves centered at the rather large sharp corner,  $K$ , of the wall.

Continuation of the magnitude of the set of expansion waves enlarges the magnitude of the turn and of the fan to the largest possible thermodynamic turn shown in figure 9, where the ambient temperature at the end of the expansion is zero.

The flow fields depicted in figures 8 and 9 are all assumed to have no boundaries other than the corner-shaped turn, that can be extended to larger and larger turn angles until the Mach number of the expanding stream cools the stream to absolute zero temperature. This “largest possible turn” of the oncoming stream occurs with a turn that is just large enough to cool the air to the point where the temperature of the airstream becomes zero absolute. As a consequence, the set of Mach waves that began as vertical lines (at the entry to the flow field where the Mach number is one,  $M_a = 1$ ), and at the end the expansion wave where the temperature is absolute zero, and the speed of sound is zero. This idealized theory then indicates that the maximum stream turning angle and velocity that can be achieved, for  $\gamma_a = 1.4$  and for a given stagnation temperature,  $T_{ao}$ , is where the streamline and the Mach lines coincide. At that point, the Prandtl-Meyer turning process predicts an angle of turning of about 220.4 degrees (e.g., Courant and Friedrich (ref. 13). Further deflection of the wall leads to a vacuum cavity that is empty, as indicated in figure 9 as a region of cavitation.

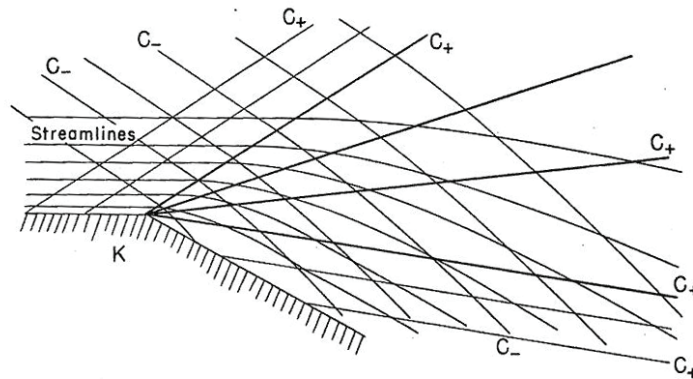


Figure 8. Centered modest-angle Prandtl-Meyer expansion fan for air (from ref. 13, Courant and Friedrichs, fig. 16, p. 277).

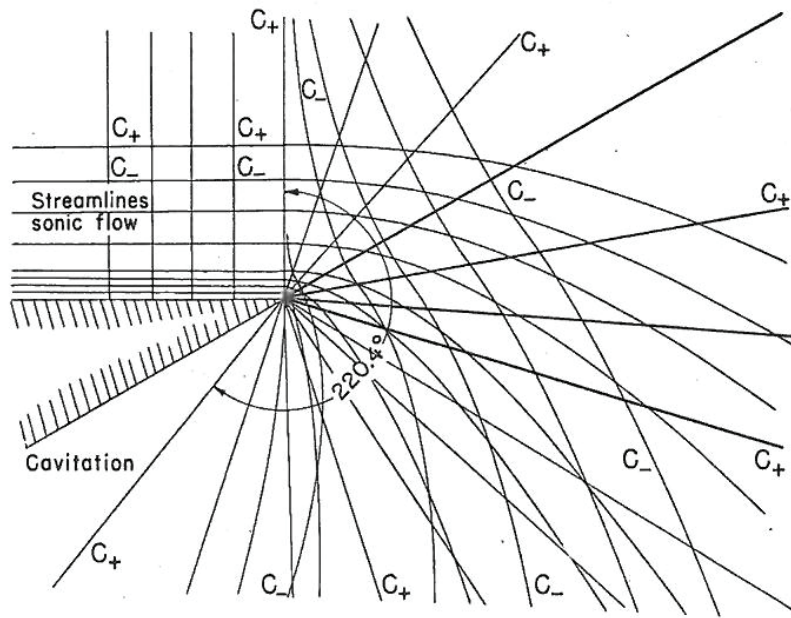


Figure 9. Complete or maximum theoretical centered angular expansion possible when stream around corner is composed of air with ratio of specific heats of 1.4 (from ref. 13, fig. 17, pp. 278; also see Liepmann and Puckett (ref. 12) p. 216ff). Note that if the turn in flow-direction angle exceeds the thermal energy available in the air (in this case, a temperature limit that allows only a  $220.4^\circ$  angular turn) it is labeled here by the word “cavitation” to indicate that turning angles do have a limit. In practice, maximum turn angles are usually limited by flow separation in the viscous boundary layers on the walls of wind tunnel nozzles and on aircraft lifting surfaces.

#### F. Method of Characteristics—Utilization of Mach Waves to Analyze Two- and Three-Dimensional Supercritical Flow Fields

The next advancement to be described in the ability to compute the structure of supercritical two- and three-dimensional flow fields is the Mach wave. The incremental Mach wave has been extensively used to build a flow-field solution on a mesh throughout the flow field of interest. A Mach wave derived solution provides parameters for the velocity and stream direction at locations where Mach waves intersect. The method was developed for supersonic flow fields in the early 1900s, and became a much used tool for the design of nozzles for supersonic wind tunnels and for the prediction of the aerodynamic loads on two-dimensional and axially-symmetric bodies (e.g., refs. 11–15 and 21–26). As indicated in some of the texts on the method, the paths of the Mach waves in the flow field, and the messages they transmit along their trajectories, are shaped during the computations to maintain their local Mach wave character as the structure develops. Therefore, iterations are required in the computations. Although the method is both reliable and accurate, the method was never automated for use on high-speed computers because the flexible and irregularly shaped Mach wave lines, and the streamlines in the flow field, bend in the computational mesh so that they are not an easy programming task

(e.g., fig. 10). The method of characteristics as a tool for the analysis of supercritical flow fields does not only provide an intuitive understanding of the fluid dynamics going on in supercritical gas streams, but also provides remarkably accurate theoretical data for the loads on nozzles for supersonic wind tunnels and on aircraft shapes moving through the atmosphere at a wide range of supersonic Mach numbers (e.g., refs. 11–15 and 21–26).

One of the first uses made by NACA of the method of characteristics was to design the shapes of nozzles and diffusers for supersonic wind tunnels being built in the 1940s and 1950s (refs. 12–15).

A second use for the method of characteristics was the computation of some calculations for the velocity and drag of axially symmetric bodies at a wide range of Mach numbers. Figure 11 presents an example of the computational mesh that was used. In the study (refs. 25, 26), the computations were made by use of a slide rule on a large drafting table so that theoretical information could be obtained on aerodynamically shaped bodies as a beginning study to accumulate design data for flight of vehicles up to and near orbital velocities. As a part of the study, the flow fields chosen for analysis were designed so that the cases calculated would test the accuracy and reliability of the hypersonic similarity rule theorized by Hayes (ref. 27). The hypersonic similarity rule was found to be more accurate than expected, and to be of use in the design of high-speed vehicles.

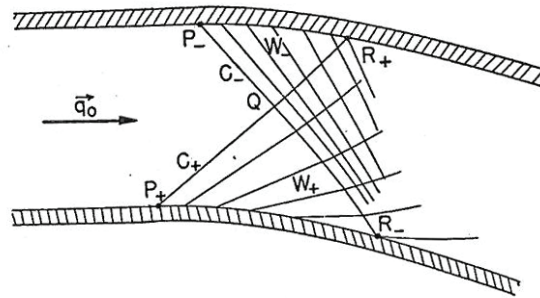


Figure 10. Supersonic flow field at bend in duct as analyzed by method of characteristics. Example illustrates how two families of Mach waves interact with each other to develop the two-dimensional form of the flow fields (from ref. 13, fig. 21, p. 282).

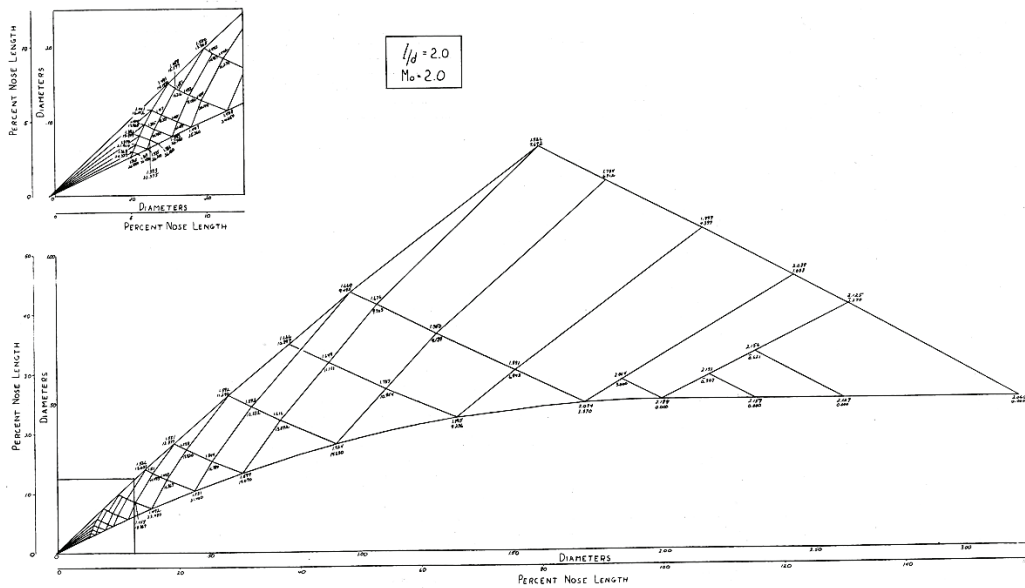


Figure 11. Reduced-size photograph of typical 30-in. by 8-ft worksheet used to carry out computations (refs. 24, 25) by use of the method of characteristics to determine the flow field around an axially symmetric ogive-cylinder of length/diameter ratio = 2.0, in an airstream moving at twice the speed of sound (Mach number = 2). Lines drawn are Mach waves used as part of the method of characteristics to compute the flow-field structure shown in the figure. Numbers on top or upper side of Mach wave intersections are local Mach number, and lower numbers are local stream angle.

## VIII. ADAPTATION OF MACH WAVE CONCEPT FOR STREAMS OF AIR TO SUPERCRITICAL STREAMS OF ELECTRON GAS

### A. Overview

The Mach wave type of analysis for supercritical streams of air has been developed and illustrated in the foregoing text. A similar application will now be made for streams of charged particles like electrons. As pointed out in several of the foregoing sections of this paper, the differential equations and pressure-wave (Mach wave) concept are the same except for the difference in the gas constants for the density and pressure relationships of the two gases. Both analyses are based on parameters like the speed of a small disturbance wave, which, in air, corresponds to the speed of sound. Another difference is that the response of air to pressure and density types of disturbances is based on parameters like molecular motions and thermodynamic parameters, whereas the gas-like characteristics of electron gases are totally based on the repulsion-type of forces, because the electron particles are assumed to have negligible random motions relative to each other. The characteristics of the two flow-field channels needed to bring about the transition of the flow-field velocities from subcritical to supercritical must be designed so that their pressure flow fields move with the aerodynamic elements of the stream. In contrast, streams of charged particles are presently usually driven by use of force fields that are fixed to a

laboratory frame of reference, making acceleration of stream elements beyond supercritical stream velocities much more difficult.

## B. Adaptation of Mach Wave Concept for Air to Electron Gas

The aerodynamic problem described in the previous section for streams of air is now adapted so that it can be applied to the same externally shaped flow fields, when the gas is made of electron particles. In order to emphasize the similarities in the two flow fields, the nomenclature used in figure 7 to model the Mach wave concept in a supercritical stream of air has been revised in this section to apply to electron gas streams as shown in figure 12 by simply changing the names of the nomenclature to begin with an “e”—thus converting the same figure from an illustration for supercritical streams of air to one for supercritical streams of electrons.

In this section, the transfer of an aerodynamic flow-field model to another in an electron stream is made to indicate how the development of a Mach wave relationship for air can be adapted to supercritical streams of electrons. The process begins by changing the nomenclature in figure 7 to the one shown in figure 12 by simply adding an “e” to the subscripts used in figure 7 for supercritical streams of air. No other adjustments are needed to make the change. As a result, the relationship between  $dV_e$  and  $d\theta_e$  may be written as

$$dV_e/V_e = \sin \beta_e d\theta_e / \cos \beta_e = \tan \beta_e d\theta_e = d\theta_e (M_e^2 - 1)^{1/2} \quad (12a)$$

or, when the variables are gathered according to function, as,

$$d\theta_e = dV_e / [V_e (M_e^2 - 1)^{1/2}] \quad (12b)$$

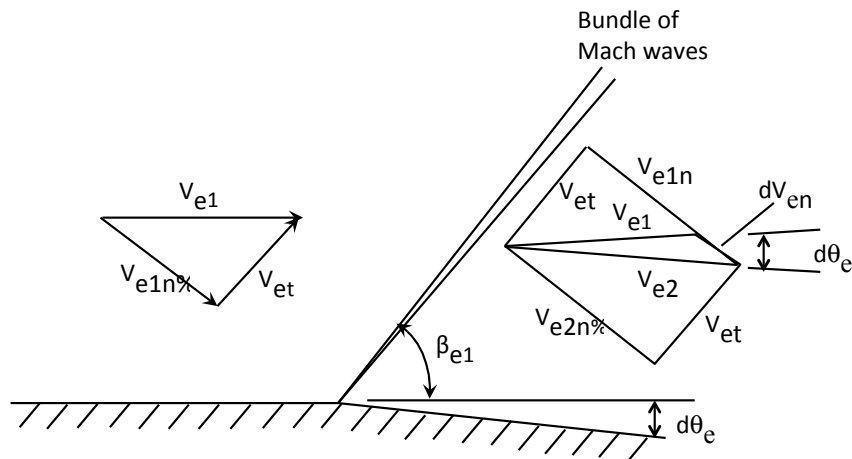


Figure 12. Copy of figure 7 with revised labels (subscript ‘e’ added) to indicate that the figure and the text now apply to supercritical streams composed of electrons rather than air. Vectors and angles were not changed because they still apply in concept, but not necessarily in the same relative magnitudes.

The subscript '1' has been eliminated from  $\beta_{e1}$  because the upstream and downstream Mach angles are assumed to be about the same. The angular change in the flow direction,  $d\theta_e$ , is then a function of the velocity,  $V_e$ , and its increase,  $dV_e$ , brought about by the action of the Mach wave, and by the speed of sound parameter,  $a_e$ , that is contained in the Mach number as  $M_e = V_e/a_e$ .

### C. Use of Reservoir Conditions for Electron Gas to Integrate Mach Wave Relationship

The chore is now to find definitions for reservoir conditions so that the various parameters in Eq. (12b) can again all be related to a common variable, and the Mach wave relationship integrated. Such a process cannot parallel the one used by Prandtl and Meyer, but must be one based on the parameter,  $d_e$ , the distance between electron centers, and not to a stagnation temperature,  $T_0$ . A similar reservoir relationship will now be developed for an electron gas.

Assume that the velocity, pressure, and density of the electron gas make up a total pressure type of parameter related through the momentum equation to the total pressure head of the stream as

$$p_e + \rho_e V_e^2/2 = H_{e0} = \text{total pressure head} = p_{e0} = \text{constant} \quad (12c)$$

Naturally, the reservoir condition is again identified as a region where the velocity of the electron gas,  $V_e$ , in the reservoir is zero. Because stream energy is conserved and constant throughout the flow field, the total head parameter,  $H_{e0}$ , for the entire flow field must then also be constant. The relationship between the static pressure,  $p_e$ , and the velocity of the electron stream at a given place in the flow field is then given by Eq. (12c). The expressions for density, pressure, and total pressure head may be written as the dynamic pressure plus static pressure as

$$[(1/d_e)^3 V_e^2/2 + E_K^2/(d_e)^2] = H_{e0}/m_e = p_{e0}/m_e = \text{constant} \quad (12d)$$

to yield

$$V_e^2 = 2d_e^3 (H_{e0}/m_e) - 2d_e E_K^2 \quad (12e)$$

and

$$V_e dV_e = [3d_e^2 (H_{e0}/m_e) - E_K^2] dd_e \quad (12f)$$

It is noted that Eqs. (12d)–(12f) now yield expressions for the stream velocity,  $V_e$ , in terms of known quantities and the electron spacing parameter,  $d_e$ , which becomes the parameter to be used to integrate the differential equation for a numerical solution to the problem for the supercritical flow of an electron gas around a corner. The remaining expression,  $(M_e^2 - 1)^{-1/2}$  may be written as

$$M_e^2 - 1 = V_e^2/a_e^2 - 1$$

where,  $V_e^2 = [2d_e^3 (H_{e0}/m_e)] - 2E_K^2 d_e$ ,

and  $a_e^2 = E_K^2/d_e^2$  so that

$$M_e^2 - 1 = \{[2d_e^3 (H_{e0}/m_e)] - 2E_K^2 d_e\} / \{E_K^2 / d_e^2\} - 1$$

$$M_e^2 - 1 = \{[2d_e^5 (H_{e0}/m_e)E_K^2] - 2d_e^3\} - 1$$

so that the foregoing equation may be written as,

$$[M_e^2 - 1]^{-1/2} = [\{[2d_e^5 (H_{e0}/m_e)E_K^2] - 2d_e^3\} - 1]^{-1/2} \quad (12g)$$

to complete the expressions needed to numerically evaluate the differential equation derived previously as

$$d\theta_e = (dV_e/V_e)/(M_e^2 - 1)^{1/2} \quad (12h)$$

Insertion of the foregoing derived quantities into the differential equation yields an expression between the increments in the flow deflection angle to the variable,  $d_e$ , the spacing of electron centers as it increases in magnitude with the flow deflection angle,  $\theta_e$ . The equations to be used in the computations then become

$$d\theta_e = (dV_e/V_e)(M_e^2 - 1)^{-1/2} \quad (12j)$$

$$V_e^2 = 2d_e^3 (H_{e0}/m_e) - 2d_e E_K^2 \quad (12k)$$

$$V_e dV_e = [3d_e^2 (H_{e0}/m_e) - E_K^2] dd_e \quad (12l)$$

$$[M_e^2 - 1]^{-1/2} = [\{[2d_e^5 (H_{e0}/m_e)E_K^2] - 2d_e^3\} - 1]^{-1/2} \quad (12m)$$

These four differential equations make it possible to rewrite the equations originally written in terms of  $V_e$  and  $M_e$  to be written in terms of the parameter,  $d_e$ , the distance between electron centers. The stream deflection angle,  $\theta_e$ , is now written in terms of only the separation distance between the centers of electrons,  $d_e$ , as

$$d\theta_e = [3d_e^2 H_{e0}/m_e - E_K^2] [\{[2d_e^5 (H_{e0}/m_e)E_K^2] - 2d_e^3\} - 1]^{-1/2} dd_e \quad (12n)$$

or

$$d\theta_e/dd_e = [3d_e^2 (H_{e0}/m_e) - E_K^2] / [\{[2d_e^5 (H_{e0}/m_e)E_K^2] - 2d_e^3\} - 1]^{1/2} \quad (12o)$$

Computations were not carried out for the foregoing situation because typical conditions to be used in an example were obscure.

## **IX. OBSERVED STRUCTURE OF ROCKET-EXHAUST PLUME AS FUNCTION OF ALTITUDE**

### **A. Background**

The foregoing corner-expansion, or Prandtl-Meyer, solutions provide quantitative information on the structure of the flow fields pictured in figures 8 and 9. These flow fields only occur in actual situations when the pressures in the flow field at the downstream end or exhaust outlet of the high-velocity flow fields are low enough so that stream expansion is not hindered nor overpowered by the pressure fields within the channel. In wind tunnels, the low-pressure conditions at downstream ends of models and nozzles for supercritical exhaust streams are usually obtained by use of vacuum pumping equipment that typically exceeds the amounts that were first estimated as needed, according to approximate conditions that were idealized in the theory. Stream failure or interference from downstream pressures has often been the problem with equipment malfunction and has usually been cured by addition or enhancement of pumping equipment at the exit of the high-speed end of the stream. That is, the remedy for failing supercritical stream structures was usually found at the downstream end of the wind tunnel stream where the experimental pressure had to be lowered further to meet the needs of the desired high-velocity stream.

### **B. Time-History of Rocket Exhaust Plume as Function of Altitude**

The following observation was made one evening of a rocket launch that was primarily upward and began somewhere near southern California. The mostly upward flight path of the rocket passed just west of overhead of the author's home on a nearly vertical, slightly south-to-north flight path. The observation is reported here because it illustrates how the reduction of atmospheric pressure with altitude influenced the flow field that surrounded the flow field of the rocket nozzle. In fact, the reduced pressures associated with altitude appear to have enabled the efficiency of the propulsion system of the rocket to increase substantially as altitude increased. That is, the improvement in efficiency experienced by the flow field of the rocket exhaust system was brought about by the reduction in the "back pressure" of the atmosphere as altitude increased. The improvement with reduced back pressure on the quality of the flow field applies not only to the performance of rocket nozzles, but also to that of high-velocity wind tunnel streams. The observation is of interest because it illustrates how the quality of the observed flow field is increased for both rocket and wind tunnel performance and it illustrates how the efficiency and shape of rocket exhaust plumes are improved by remarkable amounts with decreasing atmospheric, or back pressure, as the altitude of the rocket increases; that is, the presence of back pressure that "interferes" with the quality of the rocket exhaust stream is large at low altitudes, but approaches zero at high altitudes. The event to be described provides an example of a situation where the "back pressure" of the atmosphere functioned as the controlling parameter for the structure of the rocket exhaust plume shed by a rocket flow field as it responds to the decreasing back pressure of the atmosphere as the altitude of the rocket increases. The observations emphasize the role of "back" pressure in the flow field around, in, and near, the aft or exhaust end of rocket nozzles or of wind tunnel circuits, and its role as a function of altitude to provide control over flow-attachment boundary conditions. The ability to observe the shape of

the rocket exhaust plume during most of its time in the atmosphere provided an excellent example of an exhaust flow field as a function of altitude, which corresponds to flow-field back pressure at the downstream ends of high-velocity wind tunnels.

The observation of the rocket flight was made from the author's home as a rocket rising from below the horizon along a nearly vertical trajectory. The visible trajectory appeared to be along an upward (nearly vertical) and northerly flight path that began in southern California and left the atmosphere somewhere north and west of the San Francisco Bay Area. Because the event occurred in early evening, the setting sun just over the horizon provided "backlight" for the rocket, its flow field, and exhaust plume. As a result, the back lighting clearly indicated the shape of the bow shock wave of the rocket itself, and of its exhaust plume throughout its flight through the part of the atmosphere that could be labeled as perceptible. The part of the trajectory observed was from just above the horizon to high altitudes where the flow field of the rocket and its plume became too faint and too small to see clearly. The nearly vertical trajectory was sloping slightly in a northerly direction. The structure of the exhaust plume appeared visually and theoretically to be primarily influenced by the decreasing pressure of the atmosphere as the altitude of the rocket increased. At the beginning of the observation, the apparent size of the rocket, its bow shock wave, and its exhaust plume occupied about one-third to one-fourth of the south-western field of view. Because the exhaust plume became larger with time, the entire flow field of the exhaust plume did not seem to grow much as a function of time, but the view of the rocket body itself appeared to shrink considerably with time as it rose in altitude, and with distance (mostly altitude) from the observer.

The event began with an excellent view of the classic shape of the exhaust plume as it exited the rocket nozzle at low altitudes as a slender exhaust stream typically observed behind rockets at low altitudes. The initial low-altitude observation clearly indicated that the exhaust plume was confined to a slender stream of flame and exhaust products that followed almost completely and directly behind the body of the rocket. Also, during that time, the bow shock wave was initially attached at the point of the nose of the rocket, and then sloped rearward as if the rocket plume did not influence the shape of the bow shock wave. At that time, the flow field appeared just like those seen in photographs, newsreels, and publications. As the rocket and its flow field rose further above the horizon, the low-altitude flow-field structural components changed slowly from an exhaust plume confined to a region directly behind the rocket body to an exhaust plume that flared out radially more and more to form a plume of larger and larger diameter and length compared with the length and size of the rocket body. Similarly, as the altitude increased, the bow wave, which had been attached to the nose of the rocket and followed somewhat the shape of the rocket body, began to widen into larger and larger angles that continued to be centered about the rocket and its exhaust plume. It also then became apparent that the exhaust stream from the rocket nozzle had not only began to flare out or widen considerably so that the edge of the plume did not travel directly rearward, but also made what appeared to be an 180-degree turn so that the exhaust stream flowed forward from its exit at the nozzle and along the side of the body of the rocket to a "separation point" where the rocket gases then flowed radially, to considerably enlarge to move the bow shock wave forward of the combined rocket body and exhaust plume. From that altitude onward, the rocket plume served as the exterior of the "apparent" shape of the body of the rocket, and its flow field as a whole, so that the bow became detached from the nose of the rocket body and moved steadily farther and farther ahead of the rocket. The flow field of

the exhaust plume continued to increase in size as the size of the rocket body appeared to shrink (to become smaller and smaller) in size, so that the rocket plume began to dominate the entire flow field. A slight glow of the rocket exhaust gases (probably because of continued combustion) continued to show the relative size and locations of the visually fading rocket body, and the exhaust plume, until the entire flow field and rocket became too small and indistinct to be of use.

The most important feature of the observed launch was the axially-symmetric expansion of the rocket plume from a slender, mostly downward and rearward direction at low altitude and high back pressure, to end with the outside surface of the exhaust plume making an 180-degree turn around the rim of the base of the rocket nozzle, up along the outside of the rocket body to a region far ahead of the rocket itself. The example observed indicates that large flow-turning angles actually do occur in the flow fields of rocket-exhaust plumes when they have a low enough back pressure (e.g., the high vacuum of space) from the surrounding (atmospheric) pressure which becomes negligible at high altitudes in comparison with the total pressure head of the rocket exhaust plume.

The foregoing observation of a rocket launch example indicates that it is important to 'overestimate' the need for high capacity and robust laboratory vacuum systems to provide adequate downstream vacuum flow systems for the supercritical flow fields being discussed here.

## **X. CONCLUDING REMARKS**

The foregoing text presents information that supports the concept that an analogy can be constructed between supersonic wind tunnels and charged-particle accelerators. Because supersonic wind tunnels and modern aircraft are well established, highly successful pieces of equipment, it is suggested here that the analogy serves to provide information from the technical area developed for supersonic flow fields to the design of charged-particle accelerators. The information provided here is intended as a guide on how to adapt tools and technology from the field of sub- and supersonic aerodynamics to the design of charged-particle accelerators in order to increase their performance capabilities. In particular, the paper presents an analysis of the characteristics of the two flow-field channels that are needed to bring about the transition of flow-field velocities from subcritical to supercritical. It is pointed out that the channels for supersonic flow fields are designed so that their pressure flow fields move with the aerodynamic elements of the stream. In contrast, streams of charged particles are presently usually driven by use of force fields that are fixed to a laboratory frame of reference, making acceleration of stream elements beyond supercritical stream velocities more difficult. The possibility that the streams of charged particles might be accelerated to relativistic velocities, where other flow-field dynamics might occur, is not addressed.

The study began with a discussion of the hardware and flow-field structures associated with subsonic and supersonic wind tunnels. The paper then presents an analysis of the characteristics of the two flow-field channels needed to bring about the transition of the flow-field velocities from subcritical to supercritical. It is pointed out that the channels for supersonic flow fields are designed so that their pressure flow fields move with the aerodynamic elements of the stream. In

contrast, streams of charged particles are presently usually driven by use of force fields that are fixed to a laboratory frame of reference, making acceleration of stream elements beyond supercritical stream velocities much more difficult. As part of this study, the similarity of the two sets of differential equations for the two areas of research show how the two sets of sub- and supercritical flow fields appear to be similar in many respects. As a consequence, it is now necessary to find ways to transfer the concepts that have been successful in aerodynamic research into the design and development of equipment that will promote the acceleration of streams of charged particles to supercritical velocities.

The paper does not go into the details as to how to modify the equipment now associated with charged-particle accelerators or how to incorporate the concepts used for the design of high-speed wind tunnels, and aircraft now in service, into the existing technology of charged-particle accelerators. Whereas, the design technology for wind tunnels and aircraft structures are now well-defined and reliable technologies, a transfer of concepts from the aerospace environment to the design of charged particle accelerators will need further study if the lessons learned in the present paper are to be successfully applied for the increased acceleration and supercritical velocities of streams of charged particles. It is recognized that such a transfer of technology will probably require added study to properly identify and expedite the design of charged-particle accelerators in order to incorporate the necessary aerodynamic concepts discussed here. It is recommended that one of the beginning experiments consist of the development of a wind-tunnel-shaped channel like the one shown in figure 4 that has been prepared for the flow of a stream of electrons. If properly done, it appears that it should be possible to develop facilities that achieve significantly improved performance in the operation of charged-particle accelerators.

## XI. REFERENCES

1. Baals, D. D.; and Corliss, W. R.: Wind Tunnels of NASA. NASA, Office of Scientific and Technical Information Branch, Washington, D.C., NASA SP-440, 1981.
2. Penaranda, F. E.; and Freda, M. S.: Aeronautical Facilities Catalogue, Vol. 1 Wind Tunnels, NASA Scientific and Technical Information Branch, Washington, D.C., NASA RP-1132. 1985.
3. Pope, A.: Wind-Tunnel Testing: John Wiley & Sons, Inc., Chapman and Hall, Ltd., London, England, 1947, pp. 3–88.
4. von Karman, T.: The Problem of Resistance in Compressible Fluids. Reale Accademia d'Italia, Class delle Scienze Fisiche, Matematiche e Naturalia, Quinto Convegno, "Volta," Rome, 1935, pp. 222–276. (Also see Collected Works of Theodore von Karman, vol. III, no. 67, pp.179–221. Butterworths Publications Ltd., 88 Kingsway, London, W. C. 2. 1956.)
5. von Karman, T.: Compressibility Effects in Aerodynamics. Journal of the Aeronautical Sciences, vol. 8, 1941, pp. 337–356. (Also see Collected Works of Theodore von Karman, vol. IV, no. 84, pp.127–164. Butterworths Publications Ltd., 88 Kingsway, London, W. C. 2. 1956.)
6. von Karman, T.: Problem of Flow in Compressible Fluids. University of Pennsylvania Bicentennial Conf., pp. 15–39. (Also see Collected Works of Theodore von Karman, vol. IV, no. 85, pp.165–183. Butterworths Publications Ltd., 88 Kingsway, London, W. C. 2. 1956.)
7. Ashley, H.; and Landahl, M.: Aerodynamics of Wings and Bodies. Addison-Wesley Publishing Co., Inc. Reading, MA, 1965, pp. 227–244.
8. Evvard, J. C.: High Speed Aerodynamics and Jet Propulsion, Vol. VII, Part E. Diffusers and Nozzles. Aerodynamic Components of Aircraft at High Speeds. Editors: A. F. Donovan and H. R. Lawrence, 1957. Princeton University Press, Princeton, NJ, pp. 586–793.
9. Frick, C. W.: High Speed Aerodynamics and Jet Propulsion, Vol. VII, Part G. Experimental Aerodynamics of Wings at Transonic and Supersonic Speeds. Aerodynamic Components of Aircraft at High Speeds. Editors: A. F. Donovan and H. R. Lawrence, 1957. Princeton University Press, Princeton, NJ, pp. 794–832.
10. Kuethe, A. M.; and Schetzer, J. D.: Foundations of Aerodynamics. John Wiley & Sons, Inc., NY, 1950, pp.119–139.10. Liepmann, H. W. and Puckett, A. E.: Introduction to Aerodynamics of a Compressible Fluid: A GALCIT Aeronautical Series, John Wiley & Sons, Inc., NY, 1947, pp. 3–88.
11. Sauer, R.: Introduction to Theoretical Gas Dynamics. Edwards Brothers, Inc., Ann Arbor, MI, 1944, pp. 82–134.
12. Liepmann, H. W.; and Puckett, A. E.: Introduction to Aerodynamics of a Compressible Fluid: A GALCIT Aeronautical Series, John Wiley & Sons, Inc., NY, 1947, pp. 3–88.
13. Courant, R.; and Friedrichs, K. O.: Supersonic Flow and Shock Waves. Interscience Publishers, Inc., NY, 1948, pp. 247–433.
14. Shapiro, A. H.: The Dynamics and Thermodynamics of Compressible Fluid Flow, Vol. I, The Ronald Press Co., 1953.

15. Shapiro, A. H.: *The Dynamics and Thermodynamics of Compressible Fluid Flow*, Vol. II, The Ronald Press Co., 1954.
16. Rott, N: Jakob Ackeret and the History of the Mach Number. *Annual Review of Fluid Mechanics*, vol. 17, no. 1, Jan. 1985, pp. 1–10.
17. Sutton, G. W.; and Sherman, A.: *Engineering Magnetohydrodynamics*. McGraw-Hill Book Co., NY, 1965, pp. 3–69.
18. Dow, W. G.: *Fundamentals of Engineering Electronics*: John Wiley & Sons, Inc., Chapman and Hall, Ltd. Sixth Printing, London, England, 1947, pp. 376–479.
19. Humphries, S., Jr.: *Principles of Charged Particle Acceleration*. John Wiley & Sons, NY, 1986.
20. Day, C: *Physics Today Special Report: 2013 Nobel Prize in Physics*. *Physics Today*, vol. 66, no. 10, Oct. 2013, pp.17–20.
21. Sauer, R.: *Method of Characteristics for Three-Dimensional Axially Symmetrical Supersonic Flows*. NACA TM 1133, 1947.
22. Sauer, R.: *General Characteristics of the Flow Through Nozzles at Near Critical Speeds*. NACA TM 1147, 1947.
23. Syvertson, C. A.; and Savin, R. C.: *The Design of Variable Mach Number Asymmetric Supersonic Nozzles by Two Procedures Employing Inclined and Curved Sonic Lines*. NACA RM A51A19, 1951.
24. Tucker, M.: *Approximate Turbulent Boundary-Layer Development in Plane Compressible Flow Along Thermally Insulated Surfaces with Application to Supersonic-Tunnel Contour Correction*. NACA TN 2045, 1950.
25. Ehret, D. M.; Rossow, V. J.; and Stevens, V. I.: *An Analysis of the Applicability of the Hypersonic Similarity Law to the Study of the Flow About Bodies of Revolution at Zero Angle of Attack*. NACA TN 2250, 1950.
26. Rossow, V. J.: *Applicability of the Hypersonic Similarity Law to Pressure Distributions Which Include the Effects of Rotation for Bodies of Revolution at Zero Angle of Attack*. NACA TN 2399, 1950.
27. Hayes, W. D.: *On Hypersonic Similitude*. *Quarterly of Applied Mathematics*, vol. V, no. 1, April 1947.

## APPENDIX: DERIVATION OF ESTIMATE FOR PROPAGATION VELOCITY OF SMALL DISTURBANCE WAVES IN AN IDEALIZED ELECTRON GAS

### A. Introduction

The critical velocity of a compressible gas is defined as the velocity of propagation of a small disturbance compression or expansion wave through a neutral gas like air, or through a gas composed of only ionized particles. In a neutral gas, the critical velocity is the same as the speed of sound. In this appendix, a relationship is derived for the velocity of propagation of a small disturbance wave as it propagates through the structure of an idealized electron gas—that is, a formula for the “speed of sound” in an electron gas. A stream of electrons was chosen because, to the author’s knowledge, electrons have the largest electronic charge-to-mass ratio of any gas that currently can be produced. In order to further simplify the flow field being studied, it is also assumed that the magnitude of any random velocities (e.g., thermal motions) that may be present in the electron gas are negligible in comparison with their time-averaged or directed (i.e., group or flow-field) velocity.

In order to be able to define the propagation velocity of a small disturbance wave in a stationary array, or streaming system of electrons, it is assumed that the electrons are uniformly distributed over a three-dimensional lattice that has uniform square cubical spaces of a size ‘ $d_e$ ’ along each edge of the 6 sides of each cubically shaped cell in the x, y, and z directions. It is also assumed that one electron is located at the center of each of these cubical cells whose edges are defined by the lattice. A front view of the mesh is shown in figure 1A to indicate how one or more sections of the three-dimensional mesh would appear to an observer if seen in front view where the first mesh hides all of the elements stacked behind it. In such a flow-field model, the only force system acting on the distributed system of electrons consists of the repulsive forces associated with each of the uniformly distributed system of electrons. Because the spacing of the electrons is uniform in all three directions, and all of the electrons are the same, the distribution of electrons is the same everywhere and the force system is in balance. It is also assumed that the system begins as a stationary system at zero “temperature” so that the entire system is stationary before an acoustic type of wave passes through the space under consideration. After the foregoing quiescent case has been treated, the case where the electrons are all moving at a uniform velocity,  $U_{\infty e}$ , in the +x direction relative to a laboratory frame, is discussed in order to develop a momentum and an energy equation for the electron gas.<sup>2</sup>

---

<sup>2</sup> In actual practice, each of the electrons will probably not always be located at the center of each cell or square box to which it has been assigned. Instead, some thermal motion within the electron flow field would probably be present and cause the distribution to move across mesh lines to a more stable network that, for example, lies along 30°, 60°, and 90° mesh lines, much like the packing locations of a large volume of spheres. In other words, in a real situation, the electrons in the flow field will likely initially move to a more stable location so that their maximum density per unit volume provides a maximum “packing fraction” that has an oblique inter-particle force system that is more difficult to analyze than the rectangular one assumed here. Therefore, the present arrangement of electrons was chosen because of its simplicity and because a more realistic arrangement of electrons is much more complex to analyze. If the more complex model had been analyzed, the added effort would probably also produce a more complex result that would not provide much, if any, increased insight into the fluid mechanics of electron gases.

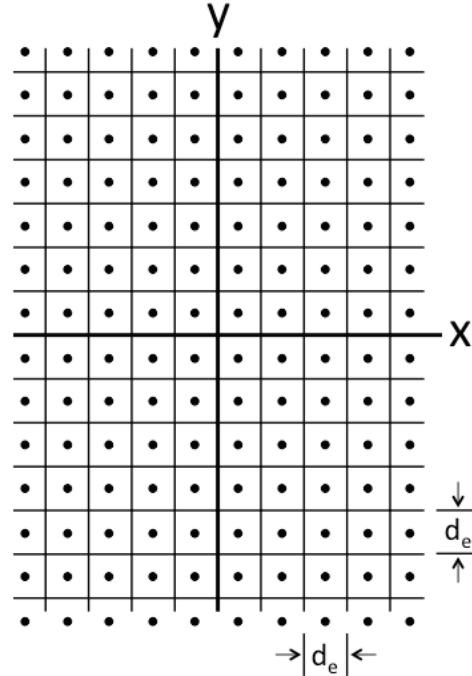


Figure A1. Diagram of a portion of the front view of theoretical mesh-spacing and electron distribution assumed for electron gas. Side and plan views are the same except for coordinate labels. Size of mesh and electron spacing are the same in all three directions, with an electron centered inside of each cube.

It is also assumed that the initial repulsion force field between all of the electrons in the lattice holds them in their original location, and that any forces due to thermal motions are negligible (especially when compared with the magnitude of any planned velocity variations in the stream as a whole). For convenience, the primary motion of the stream of lattice elements is assumed to be in the x-direction at the same velocity, so that the electrical repulsive forces on each electron are the same in all three directions, which is also the same as if the electron lattice were stationary. In the analysis presented, it is observed that the velocity of the stream as a whole does not affect the forces experienced by the electrons in the vicinity of a small-amplitude pressure wave and its propagation velocity.

Because the foregoing arrangement of electrons assumes that the electrons are all initially stationary relative to each other, a disturbance wave is assumed to consist of the streamwise displacement of one across-stream lattice layer that stretches indefinitely in the 'y' and 'z' directions. The purpose of such an analysis is to derive a relationship for the propagation velocity,  $a_e$ , of a small-amplitude disturbance wave through the lattice of electrons. The propagation velocity,  $a_e$ , for a flow field made of equally spaced electrons will be based on the same relationship used to define the propagation velocity of a small-disturbance wave through an electronically neutral gas, like air, when written as

$$a_a^2 = \partial p_a / \partial \rho_a \quad (A1a)$$

which, by use of the equation of state for air, may also be written as

$$a_a^2 = \gamma_a p_a / \rho_a = \gamma_a R_a T_a \quad (\text{A1b})$$

As a reminder, the propagation of a disturbance wave through air in a wind tunnel is assumed to depend only on the thermal motion of a mixture of gases (as described by its equation of state), which is usually about 335 m/s ( $\approx 1,100$  ft/s).

In the case of the assumed electron gas, the propagation of a small-amplitude wave through the lattice of stationary electrons is assumed here to be due only to the imbalance of the forces of repulsion produced by the irregular spacing of one y-z plane in the lattice network. That is, equations will now be derived for how fast a disturbance like a displacement of one across-stream layer of the electron lattice by a small amount,  $\delta_w \Delta$ , in the x direction will propagate through the lattice network of electrons. The equation for the propagation velocity,  $a_e$ , of a small-amplitude wave is assumed to be given by an application of Eq. (A1) written as

$$a_e^2 = \Delta p_e / \Delta \rho_e \quad (\text{A2})$$

where,  $p_e$  is a pressure type of repulsive force acting on a segment of the electron gas per square meter or, dynes/meter<sup>2</sup>, and the density of the electron gas per cubic meter is based on the mass of the number of electrons per meter<sup>3</sup> times the mass of one electron, and  $\rho_e$  is the sum of the mass of the number of electrons where  $m_e$  is the mass of one electron so that

$$\rho_e = m_e (1/d_e)^3 \quad (\text{A3a})$$

and, the pressure force per m<sup>2</sup> is given by

$$p_e = (e^2 / 4\pi K_0) [1/(d_e^2)] \quad (\text{A3b})$$

The implement in pressure,  $\Delta p_e$ , and in density,  $\Delta \rho_e$ , are used for the evaluation of the structure of the restoration force on a displaced plane of lattice-placed electrons. The restoration forces on a lattice-sized column as generated by the displaced electrons are used to determine the quantity,  $\Delta p_e$ , and the change in the density,  $\Delta \rho_e$ , of the electron gas. These two quantities are assumed to be brought about by the displacement,  $\delta_w \Delta$ , of a single plane of lattice-placed electrons. The disturbance wave is assumed to be due to the passage of an infinitesimally small compression or expansion wave. That is, as if the displacement had consisted of an infinitesimal amount,  $\delta_w \Delta$ , in the x direction (like one that might have occurred in an electronically neutral gas like air) so that the restorative force would have been related to the pressure and density changes in the gas produced by the pressure forces generated by thermal motions associated with the thermal

activity by the air molecules. In the case of the network of electrons just described, the restoring forces acting on the displaced planar lattice of electrons on the layer that extends indefinitely in the y and z directions is one of an imbalance in the repulsion forces generated by the nearby planes of electrons in the 'y' and 'z' directions.

In the model, it is the speed of propagation,  $a_e$ , of a small compression or expansion wave (a type of sound wave), that is used to simulate mathematically a pressure wave of air in a high-speed wind tunnel or in the flow of an electron gas through a channel. That is, instead of thermal motion of molecules being the "pressure force" in the fluid, as occurs in neutral gases, it is assumed here that the electrons or "particles in the stream" repel one another, because particles of the same charge repel one another. It is also assumed that the electrons in the flow-field model are all identical. The magnitude of the force between two particles is assumed to be the same as when two electrons approach each other along a common line of approach. When the weight or mass of each electron is included in the model, a type of "spring-loaded" system is constructed that facilitates an estimate to be made for the "compressibility" and/or "elasticity" of the electron gas being used in the model. It is assumed that such a model can be represented by a pressure-density relationship similar to the one that is used to model transonic and supersonic flow fields in wind tunnel airstreams.

The derivation begins with the assumption that the statically or thermally induced pressure,  $p$ , in the flow field occupied by air is replaced by the electrostatic repulsion force,  $F$ , between electrons as a function of distance between their centers in a direction along the direction of the disturbance. In order to simplify the derivation, it is assumed that the grid directions are aligned with the direction of the disturbance—presumably in the x-direction. The density of the electron gas being studied by the foregoing experiment, or fluid, as identified by the symbol,  $\rho_e$ , is specified as the mass of one electron ( $m_e = 9.11 \times 10^{-31}$  kg) times the number of electrons per meter<sup>3</sup>, and its electronic charge of one electron as,  $e = -1.60 \times 10^{-19}$  Coulombs (ref. 19) divided by the volume of the cube occupied (at its center) by an electron. The same spacing, volume, density, etc., is assumed to apply to all of the electrons in the force/pressure field and the density of the entire matrix system that makes up the "fluid" being analyzed. In particular, the fluid matrix is idealized to the point where all of the lattice locations of the electrons are located at the centers of the cubes so that they are all located one behind the other in the streamwise direction (i.e., each electron is located in front of and behind an infinite array of electrons). It is also assumed that they all remain aligned in the streamwise direction, as the electron fluid expands and contracts in volume as the disturbance wave passes. When all of the electrons are aligned in this fashion, the fore and aft forces repel each other so that the net force on each electron is zero as the electron fluid expands and contracts during its motion about the flow field, if the electron is not near an edge of the matrixes. In general, it will be assumed that the electron fluid is not near a boundary.

An estimate for the restoring force on a single displaced across-stream element of the electron lattice is now reduced to the computation of a single electron that is a part of a row of electrons that has been displaced so that it experiences a restoring force of maximum magnitude from the closest front and rear electrons, and restoring forces from the electrons in the infinite arrays of corresponding cells off to each side, and to above and below the cell being analyzed. If a cell or

cells in the lattice of electrons is disturbed from its equilibrium location, the disturbed cell will experience the largest restoring forces from nearby cells that tends to force the displaced cell, or cells, in order to restore the lattice to its original, statically stable configuration, and lessen forces from electrons further away. The restoring forces on a chosen displaced electron will now be analyzed in order to derive a speed of sound type of parameter for the electron gas that can be used to study the dynamics of an electron gas in various types of flow situations.

## B. Derivation of Equation for Speed of Propagation of Small Disturbance Waves

The first tool needed is an expression for the magnitude of the repulsion force experienced by two electrons spaced “ $d_e$ ” units (or  $\Delta x$  units) apart in order to derive an expression for the speed of propagation of a small disturbance wave through the gas as

$$a_e^2 = \Delta p_e / \Delta \rho_e = (\text{restoring force per unit cross-sectional area of lattice box}) / (\text{density of electron mass per unit of volume of lattice box}) \quad (\text{A4})$$

or, similarly,

$$a_e^2 = \Delta p_e / \Delta \rho_e = (\text{force that arises per unit area of lattice box in stream direction when electron is displaced by disturbance wave}) / (\text{difference in mass per unit volume of electron in lattice box before, during and after disturbance wave}) \quad (\text{A5})$$

Expressions for ‘pressure/density’ or ‘force-per-unit-area/density-per-unit-volume’ relationships are now developed by use of information listed in several books on aerodynamic theory (refs. 10–15). If an electron is displaced forward from its equilibrium location by a small increment in the x-direction, the increased repulsive force that is pushing the displaced electron back into its equilibrium location in order to restore the displaced electron to its original or equilibrium location, is given by

$$F_{\text{fore}} = (e^2 / 4\pi K_0) [1 / (d_e - \delta_w)^2] \quad (\text{A6})$$

The magnitude of the restoring force from the nearest following electron is given by

$$F_{\text{aft}} = (e^2 / 4\pi K_0) [1 / (d_e + \delta_w)^2] \text{ where, } 1/4\pi K_0 = 8.988 \times 10^9 \text{ [(newton-m}^2\text{)/(amp}^2\text{-sec}^2\text{)]} \quad (\text{A7})$$

where,  $1/4\pi K_0 = 8.988 \times 10^9$  [(volt-m)/(amp-sec)], and the distances  $d_e$  and  $\delta_w$  are in meters, or fractions of one.

If the displacement is small, the increment of restoring force from the nearest aft and the nearest front electron lattice, the two forces will be opposite in sign and nearly equal in magnitude, and may be combined as

$$\Delta F_{\text{restore}} \approx (e^2 / 4\pi K_0) [\pm 4\delta_w / d_e^3] \quad (\text{A8})$$

where the  $\pm 4$  multiplier is used instead of  $\pm 2$  because it is assumed that the front and rear restoring forces are equal in magnitude and that both contribute equally to the magnitude of the restoring force (i.e., in the same direction and not in opposition to each other).

In order to develop the information for the speed of sound Eq. (A3),  $a_e^2 = \Delta p_e / \Delta \rho_e$ , it is now assumed that the parameter derived as  $\Delta F_{\text{restore}}$  is an estimate of the quantity  $\Delta p_e$  in the equation for the speed of propagation of a small disturbance wave through an electron gas so that  $\Delta p_e$  is approximated by the expression for  $\Delta F_{\text{restore}}$  as

$$\Delta p_e \approx \Delta F_{\text{restore}} \approx (e^2 / 4\pi K_0) (\pm 4 \delta_w / d_e^3) \quad (\text{A9})$$

The next step in the derivation process is to determine an estimate for the change in density of the cell as affected by the small disturbance wave as it passes through the region. Evaluation of the estimate begins with an estimate for the mass density,  $\Delta \rho_e$ , where the subscript 'e' is again used to signify that the density value is associated with the one electron located inside of each of the cells designated as square-block containers for the electrons that are in the flow field of the stream being analyzed. The mass of a single electron is denoted by the symbol,  $m_e$ , and the size of each edge of each of the cells in the lattice where an electron resides is again denoted by  $d_e$ , and the change in the size of the disturbed side of each cell due to the passage of a small amplitude compression wave is designated by  $\delta_w$ . The initial density of a typical cell is first defined as

$$\rho_e = m_e / d_e^3 \quad (\text{A10})$$

When the small disturbance wave interacts with a cell and compresses (or expands) its three-dimensional size from  $d_e$  downward to  $(d_e - \delta_w)^3$ , the volume of the cell reduces to

$$V_e = +(d_e \pm \delta_w)^3 = (d_e^3 \pm 3 d_e^2 \delta_w + 3 d_e \delta_w^2 \pm \delta_w^3) \quad (\text{A11})$$

where it is assumed that, because of their small size relative to fluid motions, all three sides of the cell size for each electron, because of the change in pressure, will shrink and expand equally along all three axes. The density may then be written as

$$\rho_e = m_e / [(d_e \pm \delta_w)^3] = m_e / [d_e^3 \pm 3 d_e^2 \delta_w + 3 d_e \delta_w^2 \pm \delta_w^3]$$

or, to first order in  $\delta_w$ , becomes

$$\rho_e = m_e / [(d_e \pm \delta_w)^3] \approx m_e / [d_e^3 \pm 3 d_e^2 \delta_w] = m_e / \{ d_e^2 [d_e \pm 3 \delta_w] \} = \quad (\text{A12})$$

The change in density of an element of the electron fluid is then estimated as

$$\Delta\rho_e = m_e \{1/d_e^2 [d_e \pm 3\delta_w] - 1/d_e^3\} = m_e \{1/[d_e^2 [1/(d_e \pm 3\delta_w) - 1/d_e]]\}$$

Or, to a first order change in the perturbation size of the cell due to a pressure change,

$$\Delta\rho_e = m_e \{1/[d_e^3] \{\pm 3\delta_w/(d_e - \delta_w)\} \approx \pm 3m_e (\delta_w/d_e) \quad (A13)$$

The velocity of propagation of a small compression wave may then be written as

$$a_e^2 = \Delta\rho_e/\Delta\rho_e \approx (e^2/4\pi K_0)[4\delta_w/d_e^3]/(\pm 3m_e\delta_w/d_e) \quad (A14)$$

and, because the order of accuracy of some of the parameters is questionable, the quantity 4/3 is set equal to 1.0, so that the speed of sound expression may be reduced to

$$a_e^2 \approx (e^2/4\pi K_0 m_e d_e^2) \quad (A15)$$

or

$$a_e \approx (e^2/4\pi K_0 m_e)^{1/2}/d_e \quad (A16)$$

Equation (A16) indicates that the propagation velocity of a small amplitude disturbance wave is inversely proportional to the only controllable variable, namely,  $d_e$ , the size of each side of the lattice cubes that enclose each electron. The magnitude of the expression is found by combination of the numerical values of the components of the parameters inside of the square root as given by various books (refs. 17 and 19) as

$$e = 1.60207 \times 10^{-19} \text{ Coulomb} = 1.60207 \times 10^{-19} \text{ amp-sec} \quad (A17)$$

$$(4\pi K_0)^{-1} = 8.988 \times 10^{+9} [(\text{Newton-m}^2)/(\text{amp}^2\text{-sec}^2)]$$

or, because  $[(\text{Newton-m}^2)/(\text{amp}^2\text{-sec}^2)]$  may be written as  $(\text{volt-m})/(\text{amp-sec})$ , the quantity becomes  $(4\pi K_0)^{-1} = 8.988 \times 10^{+9} (\text{volt-m})/(\text{amp-sec})$ .

Lastly, the mass of the electron is given by  $m_e = 9.11 \times 10^{-31} \text{ kg}$ , so that the velocity of propagation of a small disturbance wave through an electron gas may be written as

$$a_e^2 \approx (e^2/4\pi K_0 m_e)/d_e^2 \approx \{[1.60207 \times 10^{-19} \text{ amp-sec}]^2 [8.988 \times 10^{+9} (\text{Newton-m}^2)/(\text{amp}^2\text{-sec}^2)]$$

$$[1 \text{ kg-m/sec}^2\text{-Newton}]/[9.11 \times 10^{-31} \text{ kg}]\}^{1/2}/d_e^2$$

where the quantity,  $(e^2/4\pi K_0 m_e)$ , has the dimensions of  $\text{m}^4/\text{sec}^2$ , which combines to yield

$$a_e^2 \approx (e^2/4\pi K_0 m_e)/d_e^2$$

$$\approx \{[2.5666 \times 10^{-38}] [8.988 \times 10^{+9}] [0.1098 \times 10^{+31}]\} / d_e^2 \text{ (m/sec)}^2$$

or

$$a_e^2 \approx 2.533 \times 10^2 / d_e^2 \text{ m}^2/\text{sec}^2$$

or

$$a_e \approx 15.92/d_e \text{ m/sec} \quad (\text{A18})$$

If the value for  $d_c$  is based on the Lorentz diameter of electrons (about  $5 \times 10^{-15}$  m, the velocity of propagation of a small disturbance wave becomes a fraction of the speed of light in a vacuum. For example, if the size of the cell is set at about  $10^{-8}$  m, the speed of propagation of a small disturbance wave is found to be about

$$a_e = a_{e)elec} \approx 1.592 \times 10^{+8} \text{ m/sec} \quad (\text{A19})$$

which is about one-half of the speed of light at  $2.998 \times 10^{+8}$  m/sec.

If the lattice size,  $d_e$ , used for the size of the box for each electron in the stream is on the order of the same as the mean free path of a molecule in a nitrogen gas stream at room conditions, the mean free path length under those conditions is on the order of about  $10^{-7}$  m. In that case, when the electron spacing is about the same amount as that for nitrogen molecules at room temperature air,  $d_{e)est} = 10^{-7}$  m, the critical velocity in such an electron gas is estimated to be about

$$a_{e)est} \approx 1.592 \times 10^{+7} \text{ m/sec} \quad (\text{A20})$$

which, when compared with the speed of light in a vacuum (i.e.,  $c = 2.998 \times 10^{+8}$  m/s), is given by

$$a_{e)est}/c \approx 0.1592 \times 10^{+8} / 2.998 \times 10^{+8} \quad a_{e)est}/c \approx 0.053 \quad (\text{A21})$$

### C. Symbolic Ratio of Specific Heats, $\gamma_e$ , for Streams of Electron Gas

The analysis for electron streams begins by writing the speed of sound in an electron stream as

$$a_e = (dp_e/d\rho_e)^{1/2} = (e/d_e)/(4\pi K_0 m_e)^{1/2} = E_K/d_e \quad (\text{A22})$$

Equation (A22) has the dimensions of velocity, m/sec, which may be calculated as

$$a_e^2 = (e^2/4\pi K_0 m_e)^2/d_e^2 = E_K^2/d_e^2$$

where the speed of propagation of a small disturbance wave through a flow field composed of electrons is given by

$$a_e \approx (e^2/4\pi K_0 m_e)^{1/2}/d_e$$

$$\approx \{[2.5666 \times 10^{-38}][[8.988 \times 10^{+9}][[1.098 \times 10^{+30}]]\}^{1/2}/d_e \text{ (m/sec)}^2$$

so that,  $E_K = (e^2/4\pi K_0 m_e)^{1/2} = 25.33 \text{ m}^2/\text{sec}$ , and

$$a_e \approx 25.33/d_e \text{ m/sec} \quad (\text{A23})$$

The speed of a small disturbance wave through an electron gas may then be either less than or greater than the velocity of light in a vacuum, depending on the magnitude of the parameter,  $d_e$ . When the electron spacing is about  $0.12 \times 10^{-8} \text{ m}$ , the parameter  $a_e$  is then about equal to the speed of light in a vacuum.

From the foregoing analysis, the relationship between the density and pressure of the electron gas is given by

$$p_e = \rho_e^{2/3} [e^2/(4\pi K_0 m_e^{1/3})^2] = 20820.0 \rho_e^{2/3} \quad (\text{A24})$$

or

$$p_e/\rho_e^{2/3} = \text{Constant} = 20820.0 \quad (\text{A25})$$

The corresponding isentropic channel flow relationship for air is given (ref. 12) by

$$p_a/\rho_a^{\gamma_a} = p_o/\rho_o^{\gamma_a} = \text{Constant} \quad (\text{A26})$$

where,  $\gamma_a = C_p/C_v$ , is the theoretical ratio of the specific heat for air a constant pressure to that of constant volume, or

$$\gamma_a = C_p/C_v = 1.400 \quad (\text{A27})$$

(where its value is measured as 1.405. If it is assumed that the two processes are equivalent, the corresponding theoretical value for the one-dimensional flow field of an electron gas would, by comparison of equations (A23) and (A24) be estimated as

$$\gamma_e = 2/3 = 0.667 \quad (\text{A28})$$

This comparison of the same thermodynamic types of equations seems to indicate that the “thermodynamic relationships” of the two gases are different enough that theoretical flow-field solutions calculated for air by use of  $\gamma_a = C_p/C_v = 1.400$  are too different to be used as reliable design information for nozzle shapes and gas-dynamic loads on equipment to be used for streams of electrons where  $\gamma_e = 0.667$ .